NAVSWC TR 91-561

USE OF KINEMATIC CONSTRAINT IN TRACKING CONSTANT SPEED MANEUVERING TARGETS

BY W. D. BLAIR G. A. WATSON
WEAPONS SYSTEMS DEPARTMENT

A. T. ALOUANI
TENNESSEE TECHNOLOGICAL UNIVERSITY

NOVEMBER 1991

NAVAL SURFACE WARFARE CENTER
Dahlgren, Virginia 22448-5000 • Silver Spring, Maryland 20903-5000

NAVSWC TR 91-561

USE OF KINEMATIC CONSTRAINT IN TRACKING CONSTANT SPEED MANEUVERING TARGETS

BY W. D. BLAIR G. A. WATSON
WEAPONS SYSTEMS DEPARTMENT

A. T. ALOUANI
TENNESSEE TECHNOLOGICAL UNIVERSITY

NOVEMBER 1991

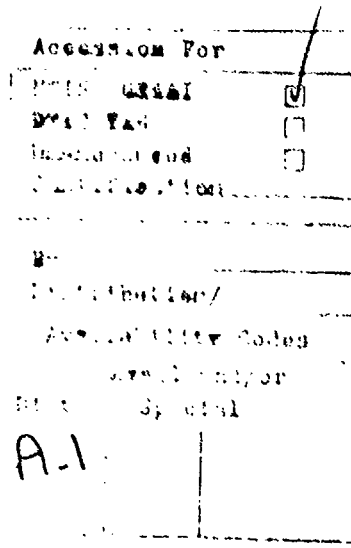

NAVAL SURFACE WARFARE CENTER
Dahlgren, Virginia 22448-5000 • Silver Spring, Maryland 20903-5000

FOREWORD

The classical problem of weapons control is predicting the future position of a maneuvering target Critical to successful prediction is the accurate estimation of the current target state. With the advent of guided weapons, the consequences of threat maneuver are reduced when accurate estimates of the target state can be obtained. Threat trends indicate that the conditions under which hostile targets can be engaged successfully are becoming more difficult to achieve; hence, any improvement in existing estimation algorithms is of critical importance.

The reported research was conducted by Mr. W. D. Blair and Mr. G. A. Watson of Naval Surface Warfare Center (NAVSWC) (Code G71) in conjunction with Dr. A. T. Alouani of the Electrical Engineering Department, Tennessee Technological University. The results of the research have advanced the state of knowledge in estimation theory and proposed a computational efficient technique for improving the state estimation for targets maneuvering through constant speed turns. The work was supported in part by the NAVSWC AEGIS Program Office and in part by the NAVSWC Independent Exploratory Development Program.

This document has been reviewed by R. T. Lee, Head, Weapons Control Division.

Approved by:

David S. Malyevac

DAVID S. MALYEVAC, Deputy Head
Weapons Systems Department

ABSTRACT

The use of a kinematic constraint as a pseudomeasurement in the tracking of constant speed, maneuvering targets is considered in this report. The kinematic constraint provides additional information about the target motion that can be processed as a pseudomeasurement to improve tracking performance. The kinematic constraint for constant speed targets is $A \cdot V = 0$, where A and V are the target acceleration and velocity vectors, respectively. In previous publications, the measurement equation for processing the kinematic constraint as a pseudomeasurement was derived by a direct application of Taylor's theorem for a first order linearization of that pseudomeasurement equation. A new formulation of the constraint equation that provides significantly better tracking performance than the previous formulation is presented along with the rationale for the new formulation. The filter using the kinematic constraint for constant speed targets is shown to be unbiased and stochastically stable. Simulated tracking results are given to show the potential for further improving the performance of a track filter through the use of the proposed kinematic constraint. Simulation studies are presented for various data rates, levels of measurement errors, and deviations in speed.

CONTENTS

CHAPTER 1
INTRODUCTION

The problem of tracking maneuvering targets has been studied extensively since the mid 1960s. One of the first works to have a significant and lasting impact on the problem was [1] where a target motion model with an acceleration that is exponentially correlated in time was introduced. In that work, a Kalman filter was utilized to estimate the position, velocities, and accelerations of the target. The rationale for the time-correlated acceleration was derived from inertial systems in that a target accelerating at time t is likely to be accelerating with similar acceleration at time $t + \tau$ for sufficiently small τ. However, the assumptions of exponentially correlated, zero-mean accelerations of [1] produced a motion model with an acceleration that decreases in magnitude during each state extrapolation. Thus, when the actual target acceleration is constant or increasing, large errors occur in the state estimates.

In the early 1970s, decision-directed tracking of maneuvering targets was introduced in [2] to respond to the demand for algorithms that could provide better tracking of targets performing high g, fast maneuvers. These decision-directed algorithms monitor the tracking errors to detect a maneuver and respond by increasing the process noise covariance and/or the dimension of the target motion model as described in [2,3,4]. While these algorithms provide good tracking performance before and after the maneuver, their performances during and immediately following the maneuver are poor. The problem with these algorithms is that the accelerations during a maneuver are not easily modeled in the sensor reference frame because they often vary irregularly with time in that frame. In [5] the accelerations were modeled in a target-oriented reference frame to reduce the problems associated with modeling the time-varying accelerations. While the algorithm in [5] provides relatively good tracking performance, the modeling and transformations that must be estimated produce a complicated algorithm.

The two-stage Kalman estimator was applied to the tracking of maneuvering targets

in [6], and a significant reduction in the convergence time after a maneuver was achieved. However, the two-stage Kalman estimator of [6] is limited to a constant acceleration model with additive white noise. Input estimation and multiple model algorithms presented in [7,8,9,10] were developed to address the problems of time-varying accelerations and convergence time after a maneuver. However, the input estimation and multiple model algorithms require significantly more computations than the previous techniques. A kinematic constraint can be utilized as additional information about the target to improve the tracking of the time-varying accelerations with a small increase in computations.

When a target's trajectory satisfies a kinematic constraint, the kinematic constraint provides additional information about the target's motion. Using the constraint removes some of the uncertainty of the time-varying accelerations and tends to force the acceleration estimates to change in a manner that is consistent with the dynamics of the target. However, including the kinematic constraint in the motion model produces a state equation with nonlinear dynamics. The use of a nonlinear state equation significantly increases the computations involved in an extended Kalman filter because the state transition must be computed on-line. Recently, the idea of introducing a kinematic constraint into the tracking process through a pseudomeasurement was proposed in [11] because nonlinearities are easier to accommodate in the measurement equation of the extended Kalman filter. The use of the constraint was shown to improve the performance of a given track filter. The improvement in the tracking performance can be attributed primarily to the reduced errors in the acceleration estimates. The constraint tends to reduce the bias or lag in these estimates when the actual acceleration is time-varying. However, using the kinematic constraint as formulated in [11] results in marginal improvement in the performance of the track filter, poor transient performance at initialization, and a track filter for which a guarantee of stability may not be achievable. In this report, a new formulation of the kinematic constraint is presented for constant speed targets, along with the rationale for the new formulation. The new formulation provides significantly better tracking performance than the one given in [11], and simulation results are given to demonstrate the relative improvement. Also, a track filter utilizing the new formulation of the kinematic constraint is shown to be unbiased and stochastically stable.

This report is organized as follows. In Chapter 2, the general problem of tracking maneuvering targets is discussed, and the kinematic constraint for constant speed targets is derived. The previously published and new formulations of the pseudomeasurement equation for the kinematic constraint are presented in Chapter 3. The bias and stability of a filter

using the new formulation are considered in Chapter 4. In Chapter 5, simulated tracking results are presented to demonstrate the improved tracking performance achieved with the kinematic constraint and document the sensitivity of the filter to data rate, measurement errors, and deviations in speed. In Chapter 6, a summary and conclusions are given along with suggestions for future research.

CHAPTER 2
BACKGROUND

In this chapter, the general problem of tracking maneuvering targets is discussed and the kinematic constraint for constant speed targets is derived. The dynamic system model of a maneuvering target in track is given by

$$\dot{X} = f(X, u, w) \tag{2.1}$$

$$Z_k = h(X_k, v_k) \tag{2.2}$$

where X is the state vector, u is the control vector, w is the process noise vector representing possible deviations in $f(\cdot)$ and external disturbances, Z_k is the discrete-time measurement vector at time k, and v_k is the measurement error vector. The dynamics of the target is a continuous-time process as shown in Eq. (2.1) where $f(\cdot)$ is a dynamical constraint that defines the motion for the target in the form of a differential equation. The dynamical constraint, which is usually unknown to the tracking system, can differ significantly between targets and change for a common target during the tracking process. As indicated by Eq. (2.2), the measurement process is discrete-time because most sensors used for target tracking record the position and/or radial velocity for a given instant in time.

While $f(\cdot)$ is usually unknown by the tracking system, the major problem with tracking maneuvering targets is that the control vector is not directly observable by the tracking system. When the target applies a control, a bias or lag develops in the estimates of the target state. The methods proposed in [8] and [9] process the position tracking errors to estimate the control vector u which produced the observed bias in the position estimates. However, for an input estimation algorithm to be effective, an extensive and usually computationally expensive maneuver detection algorithm as in [9] is required. The control can be included as acceleration in the dynamical constraint $f(\cdot)$, but the acceleration most often varies with time in such a manner that a filter model cannot be clearly identified during tracking. Thus, the target dynamics are most often modeled as linear in a Cartesian coordinate frame to simplify the filtering and reduce the computational requirements. Also, for convenience the

continuous-time dynamics are converted to a discrete-time system. As a result, the dynamics model commonly assumed for a target in track is given by

$$X_{k+1} = F_k X_k + G_k w_k \tag{2.3}$$

where $w_k \sim N(0, Q_k)$ is the process noise, F_k defines a linear constraint on the dynamics, and G_k is the process noise input matrix. The target state vector X_k contains the position (x, y, z), velocity $(\dot{x}, \dot{y}, \dot{z})$, and acceleration $(\ddot{x}, \ddot{y}, \ddot{z})$ of the target at time k as well as other variables used to model the time-varying acceleration. When the target applies a control and the time-varying accelerations are modeled incorrectly, a bias or lag develops in the estimates of the target state. While multiple dynamics models can be used as proposed in [7] and [10] to identify the best model available in the filter, identifying the exact model is not feasible because the target can apply many different control vectors to evade the tracking system. Also, since Eq. (2.3) is a linear function of X_k, the motions in the x, y, and z coordinates are often modeled as independent, while these motions are very seldom independent in the coordinate frame chosen for tracking. Therefore, additional information would be helpful to reduce the modeling error of the time-varying accelerations.

A kinematic constraint can be utilized as additional information about the target to reduce the errors in the state estimates due to time-varying accelerations and model uncertainty. Using the kinematic constraint tends to force the acceleration estimates to change in a manner that is consistent with the dynamics of the target. A kinematic constraint can be developed for use in tracking constant speed, maneuvering targets. The speed of a target is given by

$$S = (\dot{x}^2 + \dot{y}^2 + \dot{z}^2)^{\frac{1}{2}} \tag{2.4}$$

For a target moving at a constant speed,

$$\frac{dS}{dt} = 0 \tag{2.5}$$

or

$$\dot{x}\ddot{x} + \dot{y}\ddot{y} + \dot{z}\ddot{z} = 0 \tag{2.6}$$

Eq. (2.6) can be written as

$$V \cdot A = 0 \tag{2.7}$$

where the target velocity V and acceleration A are given by

$$V = [\dot{x} \quad \dot{y} \quad \dot{z}]^T \tag{2.8}$$

and

$$A = [\ddot{x} \quad \ddot{y} \quad \ddot{z}]^T \tag{2.9}$$

This kinematic constraint for constant speed targets is useful information that can be incorporated into the system state in Eq. (2.1) or used as a pseudomeasurement in conjunction with Eq. (2.2). While both approaches are conceptually feasible, the second approach is more attractive because the first restricts the state equation to be nonlinear. In the implementation of the extended Kalman filter, including nonlinearities in the measurement equation is computationally less expensive than in the state equation [11]. If the state equation is nonlinear, the transition matrix for propagating the state from time k to time $k+1$ must be computed on-line at each propagation because the transition matrix will be highly dependent on the state of the target. Computing the transition matrix on-line greatly increases the computational cost of implementing the extended Kalman filter. Thus, incorporating the kinematic constraint into the filter as a pseudomeasurement as suggested in [11] is the focus of this report.

In this report, the measurement process of Eq. (2.2) will be assumed to be linear. While most sensors used for target tracking measure the target position in spherical coordinates, the spherical measurements can be transformed into a Cartesian coordinate frame for processing as a linear function of the target state. Thus, the measurement process is given by

$$Z_k = H_k X_k + v_k \tag{2.10}$$

where Z_k is the target measurement in the Cartesian coordinate frame, H_k is the input matrix, and $v_k \sim N(0, R_k)$ is the measurement error. While the measurement errors in spherical coordinates are usually assumed to be Gaussian and uncorrelated in range, bearing, and elevation, the transformation to the rectangular coordinate frame causes the components of v_k to become nonGaussian and correlated.

A Kalman filter is often employed to filter the measurements for estimating the state of the target. When the target motion and measurements are linear and the measurement and motion modeling error processes are Gaussian, the Kalman filter provides the minimum mean-square error estimate of the target state. When the target motion and measurement models are linear, but the error processes are not Gaussian, the Kalman filter is the best linear estimator in the mean-square error sense. The Kalman filtering equations associated with the state model of Eq. (2.3) and the measurement model of Eq. (2.10) are given by the following equations.

Time Update:

$$X_{k+1|k} = F_k X_{k|k} \tag{2.11}$$

$$P_{k+1|k} = F_k P_{k|k} F_k^T + G_k Q_k G_k^T \tag{2.12}$$

Measurement Update:

$$X_{k|k} = X_{k|k-1} + K_k[Z_k - H_k X_{k|k-1}] \tag{2.13}$$

$$P_{k|k} = [I - K_k H_k] P_{k|k-1} \tag{2.14}$$

$$K_k = P_{k|k-1} H_k^T [H_k P_{k|k-1} H_k^T + R_k]^{-1} \tag{2.15}$$

where $X_k \sim N(X_{k|k}, P_{k|k})$ with $X_{k|k}$ and $P_{k|k}$ denoting the mean and error covariance of the state estimate, respectively. The subscript notation $(k|j)$ denotes the state estimate for time k when given measurements through time j, and K_k denotes the Kalman gain at time k.

The measurement update of the Kalman filter can be viewed as a weighted least-square estimation problem as discussed in [11]. For the system in Eqs. (2.3) and (2.10), the objective function to be minimized in the least-squares sense with respect to X_k is

$$J(X_k) = \frac{1}{2}[(X_k - X_{k|k-1})^T P_{k|k-1}^{-1} (X_k - X_{k|k-1}) + (Z_k - H_k X_k)^T R_k^{-1} (Z_k - H_k X_k)] \tag{2.16}$$

where $X_{k|k-1}$ is the predicted state estimate for time k based on measurements through time $k-1$, and $P_{k|k-1}$ is the covariance of $(X_k - X_{k|k-1})$. The resulting estimate of X_k that minimizes $J(X_k)$ is denoted as $X_{k|k}$. This cost function will be utilized to explain and justify the inclusion of the kinematic constraint as a pseudomeasurement. The formulation of the pseudomeasurement equation for the kinematic constraint used in [11] is presented in the next chapter along with the new formulation of the pseudomeasurement equation.

CHAPTER 3

FORMULATIONS OF THE KINEMATIC CONSTRAINT

The kinematic constraint of Eq. (2.7) can be incorporated into the Kalman filter as a pseudomeasurement through direct linearization of the constraint equation or through a modified formulation of the constraint. In this chapter, both the direct approach and the new formulation of the constraint are presented.

DIRECT LINEARIZATION

Since the kinematic constraint is a nonlinear function of the target state, it is first linearized about the predicted state $X_{k|k-1}$ as

$$V_k \cdot A_k = V_{k|k-1} \cdot A_{k|k-1} + \bar{C}_{k|k-1}(X_k - X_{k|k-1}) \tag{3.1}$$

where

$$X_k = [x_k \quad y_k \quad z_k \quad \dot{x}_k \quad \dot{y}_k \quad \dot{z}_k \quad \ddot{x}_k \quad \ddot{y}_k \quad \ddot{z}_k]^T \tag{3.2}$$

$$\bar{C}_{k|k-1} = [0 \quad 0 \quad 0 \quad \ddot{x}_{k|k-1} \quad \ddot{y}_{k|k-1} \quad \ddot{z}_{k|k-1} \quad \dot{x}_{k|k-1} \quad \dot{y}_{k|k-1} \quad \dot{z}_{k|k-1}] \tag{3.3}$$

Since

$$\bar{C}_{k|k-1}X_{k|k-1} = 2V_{k|k-1} \cdot A_{k|k-1} \tag{3.4}$$

and $V_k \cdot A_k = 0$, Eq. (3.1) can be written as

$$V_{k|k-1} \cdot A_{k|k-1} = \bar{C}_{k|k-1}X_k \tag{3.5}$$

Since the constraint has been linearized and the target motion may deviate slightly from a constant speed, the linearized constraint is modeled with an additive error as

$$V_{k|k-1} \cdot A_{k|k-1} = \bar{C}_{k|k-1}X_k + \mu \tag{3.6}$$

where $\mu \sim N(0, R_\mu)$ relaxes the constraint. With this final modification, the nonlinear kinematic constraint is in the form of a linear measurement. The cost function of Eq. (2.16)

can be augmented with Eq. (3.6) to obtain

$$J^a(X_k) = \frac{1}{2}[(X_k - X_{k|k-1})^T P_{k|k-1}^{-1}(X_k - X_{k|k-1}) + (Z_k - H_K X_k)^T R_k^{-1}(Z_k - H_k X_k) + (V_{k|k-1} \cdot A_{k|k-1} - \bar{C}_{k|k-1} X_k)^T R_\mu^{-1}(V_{k|k-1} \cdot A_{k|k-1} - \bar{C}_{k|k-1} X_k)] \quad (3.7)$$

After augmenting the measurement with the kinematic constraint, the cost function is given by

$$J^a(X_k) = \frac{1}{2}[(X_k - X_{k|k-1})^T P_{k|k-1}^{-1}(X_k - X_{k|k-1}) + (Z_k^a - L_K X_k)^T (R_k^a)^{-1}(Z_k^a - L_k X_k)] \quad (3.8)$$

where

$$Z_k^a = \begin{bmatrix} Z_k \\ V_{k|k-1} \cdot A_{k|k-1} \end{bmatrix} \quad (3.9)$$

$$L_k = \begin{bmatrix} H_k \\ \bar{C}_{k|k-1} \end{bmatrix} \quad (3.10)$$

$$R_k^a = \begin{bmatrix} R_k & 0 \\ 0 & R_\mu \end{bmatrix} \quad (3.11)$$

A Kalman filter can be implemented to minimize $J^a(X_k)$ in the least-squares sense with respect to X_k. For the filter, Eq. (2.3) serves as the state model and the measurement model is given by

$$Z_k^a = L_k X_k + v_k^a \quad (3.12)$$

where $v_k^a = [v_k \ \mu]^T$. This formulation closely parallels the one given in [11]. A new formulation for including the kinematic constraint in the filter as a pseudomeasurement is given in the next section.

NEW FORMULATION

Examining the formulation for the kinematic constraint in Eq. (3.6) shows that several modifications can be made to improve the formulation. The kinematic constraint can be linearized about the filtered state estimate $X_{k|k}$ instead of the predicted state estimate $X_{k|k-1}$. By processing the measurement Z_k before linearization, a more accurate linearization can be achieved because the filtering of Z_k reduces the error in velocity and acceleration estimates used in $\bar{C}(\cdot)$. Also, analyzing Eq. (3.5) shows that the acceleration estimates are used in $\bar{C}(\cdot)$ to observe the target velocities and the velocity estimates are used to observe the target accelerations. Since the acceleration estimates are usually less accurate than the

velocity estimates, using the acceleration estimates to observe the velocities may be counter productive. Thus, from the first two points, the kinematic constraint of Eq. (2.7) is written as

$$V_{k|k} \cdot A_k = 0 \tag{3.13}$$

where

$$V_{k|k} = \begin{bmatrix} \dot{x}_{k|k} & \dot{y}_{k|k} & \dot{z}_{k|k} \end{bmatrix}^T \tag{3.14}$$

and

$$A_k = \begin{bmatrix} \ddot{x}_k & \ddot{y}_k & \ddot{z}_k \end{bmatrix}^T \tag{3.15}$$

The $V_{k|k}$ is the filtered velocity estimate, and A_k is the actual target acceleration at time k. The kinematic constraint of Eq. (3.13) is a linear function of the elements of state vector. Since

$$V_{k|k} \cdot A_k = |V_{k|k}||A_k|\cos\theta \tag{3.16}$$

and errors in $V_{k|k}$ can produce $\theta \neq \pi/2$, $V_{k|k} \cdot A_k$ can be rather large when the magnitude of the velocity or speed is large. Thus, in order to remove the dependence of the constraint equation on the target speed, Eq. (3.13) is written as

$$\frac{V_{k|k}}{S_{k|k}} \cdot A_k = 0 \tag{3.17}$$

where

$$S_{k|k} = (\dot{x}^2_{k|k} + \dot{y}^2_{k|k} + \dot{z}^2_{k|k})^{\frac{1}{2}} \tag{3.18}$$

Since the constraint may not be satisfied exactly and $V_{k|k}$ is an estimate of the velocity, Eq. (3.18) is modeled with additive white noise to relax the rigidity of the constraint. The resulting kinematic constraint equation is

$$\frac{V_{k|k}}{S_{k|k}} \cdot A_k + \mu_k = 0 \tag{3.19}$$

where $\mu_k \sim N(0, R^\mu_k)$. The μ_k is a white Gaussian process that accounts for the uncertainty in $V_{k|k}$ and the constraint. Since the initial estimates of $V_{k|k}$ may be very poor, R^μ_k is initialized with a large value and allowed to decrease as

$$R^\mu_k = r_1(\delta)^k + r_0 \tag{3.20}$$

where r_1 is chosen large for initialization and r_0 is chosen for steady-state conditions.

The filtering equations for the new formulation of the kinematic constraint are given in the following equations where $X^c_{k|k}$ denotes the state estimate after the constraint has been applied, and $P^c_{k|k}$ is the associated state error covariance. The filtering equations are

Time Update:

$$X_{k+1|k} = F_k X^c_{k|k} \tag{3.21}$$

$$P_{k+1|k} = F_k P^c_{k|k} F_k^T + G_k Q_k G_k^T \tag{3.22}$$

Measurement Update:

$$X_{k|k} = X_{k|k-1} + K_k[Z_k - H_k X_{k|k-1}] \tag{3.23}$$

$$P_{k|k} = [I - K_k H_k] P_{k|k-1} \tag{3.24}$$

Constraint Update:

$$X^c_{k|k} = [I - K^c_k C_k] X_{k|k} \tag{3.25}$$

$$P^c_{k|k} = [I - K^c_k C_k] P_{k|k} \tag{3.26}$$

where

$$K_k = P_{k|k-1} H_k^t [H_k P_{k|k-1} H_k^T + R_k]^{-1} \tag{3.27}$$

$$K^c_k = P_{k|k} C_k^T [C_k P_{k|k} C_k^T + R^\mu_k]^{-1} \tag{3.28}$$

$$C_k = \frac{1}{S_{k|k}} \begin{bmatrix} 0 & 0 & 0 & 0 & 0 & 0 & \dot{x}_{k|k} & \dot{y}_{k|k} & \dot{z}_{k|k} \end{bmatrix} \tag{3.29}$$

Simulation results demonstrating the tracking performance of a filter using this formulation of the kinematic constraint are given in Chapter 5. The stability of the filter is considered in the next chapter.

CHAPTER 4

STABILITY AND BIASNESS ANALYSIS

The filtering problem consists of estimating the state of a stochastic dynamical system from noisy observations. One of the requirements of the estimation problem is that the system be stochastically observable. If the system is not completely observable, part or all of the state may not be extracted from the measurement information. The confidence level of the state estimates is measured by its error covariance matrix. If the error covariance matrix is not bounded, one would have no confidence in the estimates. Another issue of importance is the filter bias. A biased filter provides rather poor estimates. The purpose of this chapter is to analyze the stability and biasness of a filter using the kinematic constraint for constant speed targets as a pseudomeasurement. If including the kinematic constraint as a pseudomeasurement produces an unstable or biased filter, using it in this manner would be an inappropriate technique for improving the performance of a tracking filter.

First, some background information on the stability of stochastic systems is given. Then stochastic stability of the filter with the kinematic constraint is considered along with the biasness of the filter.

BACKGROUND ON STOCHASTIC STABILITY

This section reviews some of the definitions and theorems related to stochastic controllability, stochastic observability, and stochastic stability for linear systems. First, consider the dynamical system of a target in track as

$$X_{k+1} = F_k X_k + G_k w_k \tag{4.1}$$

$$Z_k = H_k X_k + V_k \tag{4.2}$$

where $w_k \sim N(0, Q_k)$, and $v_k \sim N(0, R_k)$.

Definition 1 [12]: The system of Eq. (4.1) is called **Controllable** in a stochastic sense

at time $k > l$ if no linear combination of the elements of the state at time k can be estimated perfectly (with no error) given only perfect knowledge of X_l. If the system is controllable for all $k > l$ then it is called **Completely Controllable.**

Theorem 1 [12]: The system of Eq. (4.1) is **Controllable** at time $k > l$ if and only if the matrix

$$\varphi(k,l) = \sum_{i=l}^{k-1} \Phi(k,i+1) G_i Q_i G_i^T \Phi^T(k,i+1) \tag{4.3}$$

is positive definite at time k, where

$$\Phi(k,i) = \prod_{j=i}^{k-1} F_j \tag{4.4}$$

and $\varphi(k,l)$ is the system controllability matrix at l.

Proof: [12] The system state at time k is given by

$$X_k = \Phi(k,l) X_l + \sum_{i=l}^{k-1} \Phi(k,i+1) G_i w_i \tag{4.5}$$

Let $c \neq 0$ be an arbitrary constant vector, then $c^T X_k$ is an arbitrary linear combination of the elements of the state at time k. The linear minimum variance, unbiased estimate of $c^T X_k$ based on X_l is

$$\widehat{c^T X_k} = c^T \Phi(k,l) X_l \tag{4.6}$$

Its estimation error is given by

$$e_k = c^T \sum_{i=l}^{k-1} \Phi(k,i+1) G_i w_i \tag{4.7}$$

The variance of the estimation error is

$$\begin{aligned} VAR[e_k] &= E[e_k e_k^T] \\ &= E\Big[c^T \sum_{i=l}^{k-1} \sum_{j=l}^{k-1} \Phi(k,i+1) G_i w_i w_j^T G_j^T \Phi^T(k,j+1) c\Big] \\ &= c^T \Big[\sum_{i=l}^{k-1} \Phi(k,i+1) G_i Q_i G_i^T \Phi^T(k,i+1)\Big] c \end{aligned} \tag{4.8}$$

An element of the estimate of $X_{k|k}$ can be perfect if and only if the variance $VAR[e_k]$ is zero for $c \neq 0$ and the matrix $\varphi(k,l)$ of Eq. (4.3) in this case is not positive definite. Therefore,

for the system to be controllable, $\varphi(k,l)$ must be positive definite. Since each term in the summation of Eq. (4.8) is non-negative definite, once the sum becomes positive definite it remains positive definite for all future times.

Q.E.D.

Definition 2 [13]: The system in Eqs. (4.1) and (4.2) is **Uniformly Completely Controllable** if there exist a positive integer N and positive constants α_1, β_1 such that

$$0 < \alpha_1 I \leq \varphi(k, k-N) \leq \beta_1 I \tag{4.9}$$

Lemma 1 [13]: If the dynamical system in Eqs. (4.1) and (4.2) is **Uniformly Completely Controllable** and $P_0 \geq 0$, then $P_{k|k} > 0$ for any $k \geq N$, where P_0 is the initial covariance matrix, and $P_{k|k}$ is the covariance matrix of the Kalman filter using the system model Eqs. (4.1) and (4.2).

Proof: See [13] pp. 238-239.

Next, the definition of stochastic observability is given along with an explanation of the requirement that the information matrix has to be positive definite in order for a stochastic system to be observable.

Definition 3 [12]: The system in Eqs. (4.1) and (4.2) is **Observable** in a stochastic sense at time l if there exists a matrix S_j such that at some $k \geq l$

$$\hat{X}_l = \sum_{j=l}^{k} S_j Z_j \tag{4.10}$$

where $\hat{X}_l$ is a minimum variance, absolutely unbiased estimate, which can be stated as

$$E[\hat{X}_l | X_l] = X_l \tag{4.11}$$

If this is true for all k, then the system is called **Completely Observable.**

Theorem 2 [12]: The system of Eqs. (4.1) and (4.2) is observable at l if and only if

$$\Theta_1(k,l) = \sum_{i=l}^{k} \Phi^T(i,l) H_i^T R_i^{-1} H_i \Phi(i,l) \tag{4.12}$$

is positive definite for some $k > l$, where $\Theta_1(k,l)$ is the information matrix of the system.

Proof: Using Eqs. (4.1) and (4.2) with $w_k = 0$,

$$Z_l = H_l X_l + v_l \tag{4.13}$$

$$Z_{l+1} = H_{l+1} F_l X_l + v_{l+1} \tag{4.14}$$

$$Z_{l+2} = H_{l+2} \Phi(l+2, l) X_l + v_{l+2} \tag{4.15}$$

$$\vdots$$

$$Z_k = H_k \Phi(k, l) X_l + v_l \tag{4.16}$$

Eqs. (4.13)-(4.16) can be written as

$$Y_k = M_k X_l + \bar{V}_k \tag{4.17}$$

where

$$M_k = \begin{bmatrix} H_l \\ H_{l+1}\Phi(l+1,l) \\ H_{l+2}\Phi(l+2,l) \\ \vdots \\ H_k \Phi(k,l) \end{bmatrix} \tag{4.18}$$

$$Y_k = [\, Z_l \quad Z_{l+1} \quad \dots \quad Z_k \,]^T \tag{4.19}$$

$$\bar{V}_k = [\, v_l \quad v_{l+1} \quad \dots \quad v_k \,]^T \tag{4.20}$$

and

$$E[\bar{V}_k \bar{V}_k^T] = \text{diag}[R_l, R_{l+1}, \dots, R_k] = \bar{R}_k \tag{4.21}$$

If an unbiased minimum variance estimate exists, it is given by in [13] as

$$\hat{X}_l = [M_k^T \bar{R}_k^{-1} M_k]^{-1} M_k^T \bar{R}_k^{-1} Y_k \tag{4.22}$$

which exists if and only if

$$M_k^T \bar{R}_k^{-1} M_k > 0 \tag{4.23}$$

For $\bar{R}_k > 0$, Eq. (4.23) is valid if M_k is a full rank matrix. Note that the system information matrix is given by

$$M_k^T \bar{R}_k^{-1} M_k = \sum_{i=l}^{k} \Phi^T(i,l) H_i^T R_i^{-1} H_i \Phi(i,l) \tag{4.24}$$

Q.E.D.

Definition 4: [13] The system in Eqs. (4.1) and (4.2) is **Uniformly Completely Observable** if there exist a positive integer N and positive constants α_2, β_2 such that

$$0 < \alpha_2 I \leq \Theta_1(k, k-N) \leq \beta_2 I \tag{4.25}$$

where $\Theta_1(k, k-N)$ isthe information matrix of the system.

Lemma 2: If the system in Eqs. (4.1) and (4.2) is uniformly completely observable and uniformly completely controllable, and if $P_0 > 0$, then $P_{k|k}$ is **Uniformly Bounded** from below for all $k \geq N$,

$$P_{k|k} \geq [\varphi^{-1}(k, k-N) + \Theta_1(k, k-N)]^{-1} \geq \left(\frac{\alpha_1}{1+\alpha_1\beta_2}\right) I, \qquad k \geq N \tag{4.26}$$

Proof: See [13] pp. 236-238.

Lemma 3: If the system in Eqs. (4.1) and (4.2) is uniformly completely observable and uniformly completely controllable, and if $P_0 \geq 0$, then the error covariance matrix $P_{k|k}$ is **Uniformly Bounded** from above for all $k \geq N$,

$$P_{k|k} \leq [\varphi(k|k-N) + \Theta_1^{-1}(k, k-N)] \leq \left(\frac{1+\alpha_2\beta_1}{\alpha_2}\right) I, \quad k \geq N \tag{4.27}$$

Proof: See [13] pp. 234-235.

Theorem 3: If the system in Eqs. (4.1) and (4.2) is uniformly completely controllable and uniformly completely observable, and if $P_0 \geq 0$, then the Kalman Filter of the system is **Uniformly Asymptotically Stable.**

Proof: see [13] pp. 240-242 and [14].

STOCHASTIC STABILITY

This section discusses the stability of the filter that uses the kinematic constraint as a pseudomeasurement. As indicated by Theorem 3, if the system with kinematic constraint is uniformly completely controllable and uniformly completely observable, then the system is uniformly asymptotically stable.

Consider the kinematic constraint of Eq. (3.19)

$$\frac{V_{k|k}}{S_{k|k}} \cdot A_k + \mu_k = 0, \tag{4.28}$$

where $\mu_k \sim N(0, R_k^{\mu})$. Eq. (4.28) may be rewritten as

$$0 = X_{k|k}^T D_k X_k + \mu_k \tag{4.29}$$

where

$$X_k = [\, x_k \quad y_k \quad z_k \quad \dot{x}_k \quad \dot{y}_k \quad \dot{z}_k \quad \ddot{x}_k \quad \ddot{y}_k \quad \ddot{z}_k \,]^T \tag{4.30}$$

$$D_k = \frac{1}{S_{k|k}} \begin{bmatrix} 0_{3\times 6} & 0_{3\times 3} \\ 0_{3\times 6} & I_3 \\ 0_{3\times 6} & 0_{3\times 3} \end{bmatrix} \tag{4.31}$$

with $0_{m\times n}$ represent the null matrix with m rows and n columns, and I_n is an identity matrix with n rows. Eqs. (4.2) and (4.29) may be rewritten as

$$\begin{bmatrix} Z_k \\ 0 \end{bmatrix} = L_k X_k + \begin{bmatrix} v_k \\ \mu_k \end{bmatrix} \tag{4.32}$$

where

$$L_k = \begin{bmatrix} H_k \\ X_{k|k}^T D_k \end{bmatrix} \tag{4.33}$$

$$\bar{R}_k = E\left\{ \begin{bmatrix} v_k \\ \mu_k \end{bmatrix} \begin{bmatrix} v_l^T & \mu_l^T \end{bmatrix} \right\} = \begin{bmatrix} R_k & 0 \\ 0 & R_k^\mu \end{bmatrix} \tag{4.34}$$

Lemma 4: If the system in Eqs. (4.1) and (4.2) is uniformly completely controllable, then the system with kinematic constraint in Eqs. (4.1) and (4.32) is also **Uniformly Completely Controllable.**

Proof: Both systems have the same controllability matrix.

Lemma 5: If the system in Eqs. (4.1) and (4.2) is completely observable, then the system with kinematic constraint is also **Completely Observable.**

Proof: The information matrix associated with the system with kinematic constraint is given by

$$\Theta(k, k_0) = \sum_{i=k_0}^{k} \Phi^T(i,k) L_i^T R_i^{-1} L_i \Phi(i,k) \tag{4.35}$$

The system is completely observable if and only if

$$\Theta(k, k_0) > 0, \quad \text{for all } k > k_0 \tag{4.36}$$

Using Eqs.(4.1), (4.33), and (4.34),

$$\begin{aligned} \Theta(k, k_0) &= \sum_{i=k_0}^{k} \Phi(i,k) \begin{bmatrix} H_i^T & D_i^T X_{i|i} \end{bmatrix} \begin{bmatrix} R_k & 0 \\ 0 & R_k^\mu \end{bmatrix}^{-1} \begin{bmatrix} H_i \\ X_{i|i}^T D_i \end{bmatrix} \Phi(i,k) \\ &= \sum_{i=k_0}^{k} \Phi^T(i,k) H_i^T R_i^{-1} H_i \Phi(i,k) + \sum_{i=k_0}^{k} \Phi^T(i,k) D_i^T X_{i|i} (R_i^\mu)^{-1} X_{i|i}^T D_i \Phi(i,k) \\ &= \Theta_1(k, k_0) + \Theta_2(k, k_0) \end{aligned} \tag{4.37}$$

where $\Theta_1(k,k_0)$ is the information matrix of the system without kinematic constraint. The $\Theta_1(k,k_0)$ is positive definite for $k > k_0$ since the original system is assumed to be completely observable. Since each term of the summation in $\Theta_2(k,k_0)$ is positive semidefinite, $\Theta_2(k,k_0)$ is positive semidefinite. Therefore,

$$\Theta(k,k_0) = \Theta_1(k,k_0) + \Theta_2(k,k_0) > 0 \tag{4.38}$$

for all $k > k_0$ and the system with pseudomeasurement is completely observable. Q.E.D.

Define

$$\bar{D}_k = \frac{1}{S^2_{k|k}} \begin{bmatrix} 0_{6\times 6} & 0_{3\times 3} \\ 0_{3\times 6} & V_{k|k}V^T_{k|k} \end{bmatrix} \geq 0 \tag{4.39}$$

where $V_{k|k}$ is the filtered target velocity vector at time k.

Assumption: Assume there exists a positive $\gamma > 0$ such that for all k

$$0 \leq \frac{1}{R^{\mu}_k}\bar{D}_k \leq \gamma G_k Q_k G^T_k \tag{4.40}$$

Theorem 4: Under the assumption of Eq. (4.40), if the system in Eqs. (4.1) and (4.2) is uniformly completely observable and uniformly completely controllable, then the system with kinematic constraint is **Uniformly Completely Observable.**

Proof: Using Eqs. (4.37) and (4.39),

$$\begin{aligned} \Theta(k,k_0) &= \Theta_1(k,k_0) + \Theta_2(k,k_0) \\ &= \Theta_1(k,k_0) + \sum_{i=k_0}^{k} \Phi^T(i,k_0)\frac{\bar{D}_i}{R^{\mu}_i}\Phi(i,k_0) \end{aligned} \tag{4.41}$$

Now, if the system in Eqs. (4.1) and (4.2) is uniformly completely observable, then using Eq. (4.25),

$$0 < \alpha_2 I \leq \Theta_1(k,k-N) \leq \beta_2 I \tag{4.42}$$

Using Eq. (4.42) in Eq. (4.41)

$$0 < \alpha_2 I + \Theta_2(k,k-N) \leq \Theta(k,k-N) \leq \beta_2 I + \Theta_2(k,k-N) \tag{4.43}$$

which implies that

$$0 < \alpha_2 I \leq \Theta(k,k-N) \leq \beta_2 I + \Theta_2(k,k-N) \tag{4.44}$$

Using Eq. (4.40),

$$\Theta_2(k,k-N) = \sum_{i=k-N}^{k} \Phi^T(i,k-N)\frac{\bar{D}_i}{R_i^{\mu}}\Phi(i,k-N)$$

$$\leq \gamma \sum_{i=k-N}^{k} \Phi^T(i,k-N)G_iQ_iG_i^T\Phi(i,k-N) \tag{4.45}$$

Thus

$$\Theta_2(k,k-N) \leq \gamma\varphi(k,k-N) \leq \gamma\beta_1 I \tag{4.46}$$

Using Eq. (4.46) in Eq. (4.44),

$$0 < \alpha_2 I \leq \Theta(k,k-N) \leq \beta_2 I + \gamma\beta_1 I \tag{4.47}$$

Define

$$\beta = \beta_2 + \gamma\beta_1. \tag{4.48}$$

Then, Eq. (4.47) can be rewritten as

$$0 < \alpha_2 I \leq \Theta(k,k-N) \leq \beta I \tag{4.49}$$

which indicates that the system with kinematic constraint is uniformly completely observable.

Q.E.D.

Lemma 6: If the system in Eqs. (4.1) and (4.2) is uniformly completely observable, $P_0 > 0$, and the assumption of Eq. (4.40) holds, then the error covariance matrix of the filter with kinematic constraint $P_{k|k}$ is **Uniformly Bounded** from below for all $k \geq N$,

$$P_{k|k} \geq [\varphi^{-1}(k,k-N) + \Theta(k,k-N)]^{-1} \geq \left(\frac{\alpha_1}{1+\alpha_1\beta}\right)I, \qquad k \geq N \tag{4.50}$$

Proof: Using Lemma 4 and Theorem 4, the system with kinematic constraint is completely uniformly controllable and completely uniformly observable. For such a system Eq. (4.50) holds by Lemma 2. Note that the lower bound of $P_{k|k}$ is a function of β, which is a function of γ.

Lemma 7: If the system in Eqs. (4.1) and (4.2) is uniformly completely observable and uniformly completely controllable, and if $P_0 \geq 0$ and assumption of Eq. (4.40) holds, then the error covariance matrix $P_{k|k}$ of the filter with kinematic constraint is **Uniformly Bounded** from above for all $k \geq N$,

$$P_{k|k} \leq [\varphi(k|k-N) + \Theta^{-1}(k,k-N)] \leq \left(\frac{1+\alpha_2\beta_1}{\alpha_2}\right)I, \quad k \geq N \tag{4.51}$$

Proof: Follows from Lemma 3.

Theorem 5: If the system in Eqs. (4.1) and (4.2) is uniformly completely controllable and uniformly completely observable, $P_0 \geq 0$, and the assumption of Eq. (4.40) holds, then the kinematically constrained filter is **Uniformly Asymptotically Stable.**

Proof: Follows from Theorem 3.

It is worth noting that the condition of Eq. (4.40) is not very restrictive in practice. Given the block diagonal structure of $\bar{D}_k$ and the fact that it is normalized, for a given R_k^μ, a large enough γ almost always exists so that Eq. (4.40) is satisfied.

BIASNESS OF KINEMATICALLY CONSTRAINED FILTER

This section considers the bias of a filter using the kinematic constraint as a pseudomeasurement. Define

$$e_{k|k} = X_k - X^c_{k|k}, \tag{4.52}$$

$$\begin{aligned} e_{k|k-1} &= X_k - X_{k|k-1} \\ &= F_{k-1}X_{k-1} + G_{k-1}w_{k-1} - F_{k-1}X^c_{k-1|k-1} \\ &= F_{k-1}e_{k-1|k-1} + G_{k-1}w_{k-1}, \end{aligned} \tag{4.53}$$

where $X^c_{k|k}$ is the filter state estimate after the kinematic constraint has been applied. Using Eqs. (4.32)-(4.34),

$$\begin{aligned} e_{k|k} &= X_k - X_{k|k-1} - K_k\left\{\begin{bmatrix} Z_k \\ 0 \end{bmatrix} - \begin{bmatrix} H_k \\ X^T_{k|k}D_k \end{bmatrix} X_{k|k-1}\right\} \\ &= e_{k|k-1} - K_k\begin{bmatrix} H_k \\ X^T_{k|k}D_k \end{bmatrix} e_{k|k-1} - K_k\begin{bmatrix} v_k \\ \mu_k \end{bmatrix} \\ &= [I - K_kL_k]\,e_{k|k-1} - K_k\begin{bmatrix} v_k \\ \mu_k \end{bmatrix} \end{aligned} \tag{4.54}$$

$$e_{k+1|k} = F_k(I - K_kL_k)e_{k|k-1} - F_kK_k\begin{bmatrix} v_k \\ \mu_k \end{bmatrix} + G_kw_k \tag{4.55}$$

$$E\left[e_{k+1|k}\right] = F_k(I - K_kL_k)E\left[e_{k|k-1}\right] \tag{4.56}$$

If $E\left[e_{k|k-1}\right] = 0$, then $E\left[e_{k+1|k}\right] = 0$.

Lemma 7: The kinematically constrained filter is unbiased if the system in Eqs. (4.1) and (4.2) is uniformly completely controllable.

Proof: Define the Lyapunov function

$$V_k = E\left[e_{k|k-1}^T\right] P_{k|k-1}^{-1} E\left[e_{k|k-1}\right] \tag{4.57}$$

It can be easily shown that

$$V_k = tr(P_{k|k-1}^{-1} E[e_{k|k-1}] E[e_{k|k-1}^T]) \tag{4.58}$$

Note that

$$\begin{aligned} P_{k|k} &= (I - K_k L_k) P_{k|k-1} \\ &= (I - K_k L_k) P_{k|k-1} (I - K_k L_k)^T + K_k R_k K_k^T \qquad (4.59) \\ P_{k+1|k} &= F_k P_{k|k} F_k^T + G_k Q_k G_k^T \qquad (4.60) \end{aligned}$$

If the system in Eqs. (4.1) and (4.2) is uniformly completely controllable, then the system with kinematic constraint is uniformly completely controllable, and $P_{k|k} > 0$, $k \geq N$, by Theorem 2. Using Eq. (4.60), $P_{k|k-1} > 0$, therefore $V_k > 0$ and V_k is a Lyapunov function.

Define the differential

$$\Delta V_{k+1} = V_{k+1} - V_k$$

Using Eqs. (4.56) and (4.57),

$$\Delta V_{k+1} = E\left[e_{k|k-1}^T\right] \{(I - K_k L_k)^T F_k^T P_{k+1|k}^{-1} F_k (I - K_k L_k) - P_{k|k-1}^{-1}\} E[e_{k|k-1}] \tag{4.61}$$

Using the matrix inversion Lemma, and assuming $R > 0$ and $G_k Q_k G_k^T > 0$;

$$\begin{aligned} &(I - K_k L_k)^T F_k^T P_{k+1|k}^{-1} F_k (I - K_k L_k) - P_{k|k-1}^{-1} \\ &= (I - K_k L_k)^T F_k^T (F_k P_{k|k} F_k^T + G_k Q_k G_k^T)^{-1} F_k (I - K_k L_k) - P_{k|k-1}^{-1} \\ &= (I - K_k L_k)^T [P_{k|k}^{-1} - P_{k|k}^{-1} [I + P_{k|k} F_k^T (G_k Q_k G_k^T)^{-1} F_k^T]^{-1} (I - K_k L_k) - P_{k|k-1}^{-1} \\ &= (I - K_k L_k)^T [P_{k|k}^{-1} - P_{k|k}^{-1} (P_{k|k}^{-1} + F_k^T (G_k Q_k G_k^T)^{-1} F_k)^{-1} \cdot \\ &\quad P_{k|k}^{-1}] (I - K_k L_k) - P_{k|k-1}^{-1} \\ &= (I - K_k L_k)^T P_{k|k}^{-1} (I - K_k L_k) - P_{k|k-1}^{-1} - (I - K_k L_k)^T P_{k|k}^{-1} \cdot \\ &\quad (P_{k|k}^{-1} + F_k^T (G_k Q G_k^T)_k^{-1} F_k)^{-1} P_{k|k}^{-1} (I - K_k L_k) \\ &= (I - K_k L_k)^T P_{k|k-1}^{-1} - P_{k|k-1}^{-1} - P_{k|k-1}^{-1} [P_{k|k}^{-1} + F_k^T (G_k Q_k G_k^T)^{-1} F_k]^{-1} P_{k|k-1}^{-1} \\ &= -L_k^T K_k^T P_{k|k-1}^{-1} - P_{k|k-1}^{-1} [P_{k|k}^{-1} + F_k^T (G_k Q_k G_k^T)^{-1} F_k]^{-1} P_{k|k-1}^{-1} \\ &= -L_k (L_k P_{k|k-1} L_k^T + R_k)^{-1} L_k - P_{k|k-1}^{-1} (P_{k|k}^{-1} + F_k^T (G_k Q_k G_k^T)^{-1} F_k)^{-1} P_{k|k-1}^{-1} \qquad (4.62) \end{aligned}$$

Eq. (4.62) is the sum of one negative semidefinite matrix and one negative definite matrix, respectively. This indicates that ΔV_{k+1} is negative definite. Hence $V_k \to 0$ as $k \to \infty$.

Therefore $E[\epsilon_{k|k-1}] \longrightarrow 0$ as $k \longrightarrow \infty$, and the filter with the pseudomeasurement is unbiased.

Q.E.D.

CHAPTER 5

SIMULATION RESULTS

This chapter presents simulation results that demonstrate the potential for improving the tracking performance of the constant acceleration Kalman filter through the use of the kinematic constraint. The simulation results are presented to document the benefits of the kinematic constraint for various data rates, measurement error variances, constraint error variances, and deviations from constant speed. This chapter is divided into four sections. The first section describes the simulation procedures employed for comparing the kinematically constrained filter with the standard unconstrained constant acceleration filter. The second section presents the target trajectories used in this study. The third section presents the simulation results for the unconstrained and kinematically constrained filters under a variety of tracking conditions. The final section summarizes the simulation results.

SIMULATION PROCEDURES

The system models used for the simulation studies are discussed in this section. A constant acceleration motion model was used since it is often used for tracking maneuvering targets. The discrete-time dynamics model for constant acceleration motion is given by Eq. (2.3) with

$$F_k = \begin{bmatrix} A & 0 & 0 \\ 0 & A & 0 \\ 0 & 0 & A \end{bmatrix} \tag{5.1}$$

$$G_k = \begin{bmatrix} B & 0 & 0 \\ 0 & B & 0 \\ 0 & 0 & B \end{bmatrix} \tag{5.2}$$

where

$$A = \begin{bmatrix} 1 & T & \frac{T^2}{2} \\ 0 & 1 & T \\ 0 & 0 & 1 \end{bmatrix} \tag{5.3}$$

$$B = \left[\frac{T^3}{6} \quad \frac{T^2}{2} \quad T \right]^T \tag{5.4}$$

$$X_k = [x_k \quad \dot{x}_k \quad \ddot{x}_k \quad y_k \quad \dot{y}_k \quad \ddot{y}_k \quad z_k \quad \dot{z}_k \quad \ddot{z}_k]^T \tag{5.5}$$

The state, X_k, contains the positions, velocities, and accelerations of each coordinate. For this simulation study, the data rate was periodic with period T being the time between successive measurements. To complete the time update portion of the Kalman filter, Q_k must be established. Since the output of the filter is in Cartesian coordinates, the model error w_k of Eq. (2.3) was modeled as a derivative of an acceleration and was assumed to have the same variance for each coordinate. Thus, with $E[w_k] = 0$ and $E\left[w_j w_k^T\right] = Q_k \delta_{jk}$,

$$Q_k = \begin{bmatrix} q_k^2 & 0 & 0 \\ 0 & q_k^2 & 0 \\ 0 & 0 & q_k^2 \end{bmatrix} = q_k^2 I_3 \tag{5.6}$$

To define the measurement equation, the measurement equation for range, bearing, and elevation, which is a nonlinear function of the state X_k, must be linearized. The measurement equation as a function of the actual target state is given by

$$Z_k = \begin{bmatrix} r_k \\ b_k \\ e_k \end{bmatrix} = \begin{bmatrix} \left(x_k^2 + y_k^2 + z_k^2\right)^{\frac{1}{2}} \\ \tan^{-1}\left(\dfrac{y_k}{x_k}\right) \\ \tan^{-1}\left(\dfrac{z_k}{\sqrt{x_k^2 + y_k^2}}\right) \end{bmatrix} + \begin{bmatrix} v_k^r \\ v_k^b \\ v_k^e \end{bmatrix} \tag{5.7}$$

where r_k, b_k, and e_k are the measured range, bearing and elevation at time k, respectively. The v_k^r, v_k^b, and v_k^e are the measurement errors for time k. The measurement errors are characterized by $E[v_k] = 0$ and $E\left[v_j v_k\right] = R_k \delta_{jk}$ with

$$R_k = \begin{bmatrix} \sigma_r^2 & 0 & 0 \\ 0 & \sigma_b^2 & 0 \\ 0 & 0 & \sigma_e^2 \end{bmatrix} \tag{5.8}$$

Let

$$h_k(X_k) = \begin{bmatrix} \left(x_k^2 + y_k^2 + z_k^2\right)^{\frac{1}{2}} \\ \tan^{-1}\left(\dfrac{y_k}{x_k}\right) \\ \tan^{-1}\left(\dfrac{z_k}{\sqrt{x_k^2 + y_k^2}}\right) \end{bmatrix} \tag{5.9}$$

Using a first order Taylor series to linearize Eq. (5.7) about the predicted state estimate $X_{k|k-1}$ gives

$$\bar{Z}_k = H_k X_k + v_k \tag{5.9}$$

where

$$\bar{Z}_k = Z_k - h_k(X_{k|k-1}) + H_k X_{k|k-1} \tag{5.10}$$

$$H_k = \left.\frac{\partial h_k(X_k)}{\partial X_k}\right|_{X_k = X_{k|k-1}} \tag{5.11}$$

The H_k matrix is given by

$$H_k = \begin{bmatrix} \frac{x_{k|k-1}}{R_{k|k-1}} & 0 & 0 & \frac{y_{k|k-1}}{R_{k|k-1}} & 0 & 0 & \frac{z_{k|k-1}}{R_{k|k-1}} & 0 & 0 \\ \frac{-y_{k|k-1}}{Rh_{k|k-1}} & 0 & 0 & \frac{x_{k|k-1}}{Rh_{k|k-1}} & 0 & 0 & 0 & 0 & 0 \\ \frac{-z_{k|k-1}x_{k|k-1}}{Rh_{k|k-1}R^2_{k|k-1}} & 0 & 0 & \frac{-z_{k|k-1}y_{k|k-1}}{R_{k|k-1}R^2_{k|k-1}} & 0 & 0 & \frac{Rh_{k|k-1}}{R^2_{k|k-1}} & 0 & 0 \end{bmatrix} \tag{5.12}$$

where

$$R_{k|k-1} = (x^2_{k|k-1} + y^2_{k|k-1} + z^2_{k|k-1})^{\frac{1}{2}} \tag{5.13}$$

$$Rh_{k|k-1} = (x^2_{k|k-1} + y^2_{k|k-1})^{\frac{1}{2}} \tag{5.14}$$

The kinematic constraint is incorporated into the track filter with the pseudomeasurement equation given in Eq. (3.19). The state estimate, $X_{k|k}$, and associated error covariance, $P_{k|k}$, from the measurement update portion of the filter are used in the constraint update process. The constrained state estimate $X^c_{k|k}$ and associated error covariance $X^c_{k|k}$ are given by

$$X^c_{k|k} = \left[I - K^c_k C_k\right] X_{k|k} \tag{5.15}$$

$$P^c_{k|k} = \left[I - K^c_k C_k\right] P_{k|k} \tag{5.16}$$

where

$$K^c_k = P_{k|k} C^T_k (C_k P_{k|k} C^T_k + R^\mu_k)^{-1} \tag{5.16}$$

$$C_k = \frac{1}{S_{k|k}} \begin{bmatrix} 0 & 0 & \dot{x}_{k|k} & 0 & 0 & \dot{y}_{k|k} & 0 & 0 & \dot{z}_{k|k} \end{bmatrix} \tag{5.17}$$

$$S_{k|k} = (\dot{x}^2_{k|k} + \dot{y}^2_{k|k} + \dot{z}^2_{k|k})^{\frac{1}{2}} \tag{5.18}$$

The only parameter involved in implementing the kinematic constraint that can be manipulated by the user is the constraint variance R_k^μ. As discussed in Chapter 3, the constraint variance has the form

$$R_k^\mu = r_1 (\delta)^k + r_0 \tag{5.19}$$

where k is the iteration number of the filter, r_1 is chosen to provide the initial constraint variance, r_0 is chosen to provide the steady state constraint variance, and δ provides the decay rate of the constraint variance. For a constant acceleration track filter, Eqs.(4.40), (5.2) and (5.6) give a relationship for determining r_0. For the case of the total target velocity being in one coordinate, Eq. (4.40) can be reduced to

$$r_0 \geq \frac{1}{\gamma T^2 q_k^2}, \tag{5.19}$$

where γ is selected by the filter designer. Note that for this case with G_k having the form given by Eqs. (5.2) and (5.4), r_0 is dependent on the sample period. The parameter γ allows the user to "tune" the constraint variance to achieve a desired reduction in the state error covariance as discussed in Chapter 4.

DESCRIPTION OF TARGET TRAJECTORIES

This section describes the three target trajectories to be used in the simulation study. The first target trajectory, Trajectory 1, shown in Figure 5.1 is a constant speed, 3 g circular trajectory that will be used to assess the tracking performance during a maneuver. In the second trajectory, Trajectory 2, shown in Figure 5.2 the target moves with constant velocity for the first 15 sec, makes a 90 degree, constant speed turn during the next 15 sec, and moves with constant velocity during the last 12 sec. The first two trajectories maintain a constant height and constant speed so that they are ideally suited for the constant speed kinematic constraint. The third target trajectory, Trajectory 3, shown in Figure 5.3 makes a constant height turn while the speed decreases at a rate of 2 m/sec^2. This trajectory will be used to assess the sensitivity of the performance of the filter utilizing the kinematic constraint to deviations in speed.

RESULTS

This section presents the simulation results for the kinematic constraint. The results for each track filter are an average of 100 Monte Carlo experiments. The Root-Mean-Square Errors (RMSE) in position, velocity, and accelerations will be used as the measure to assess

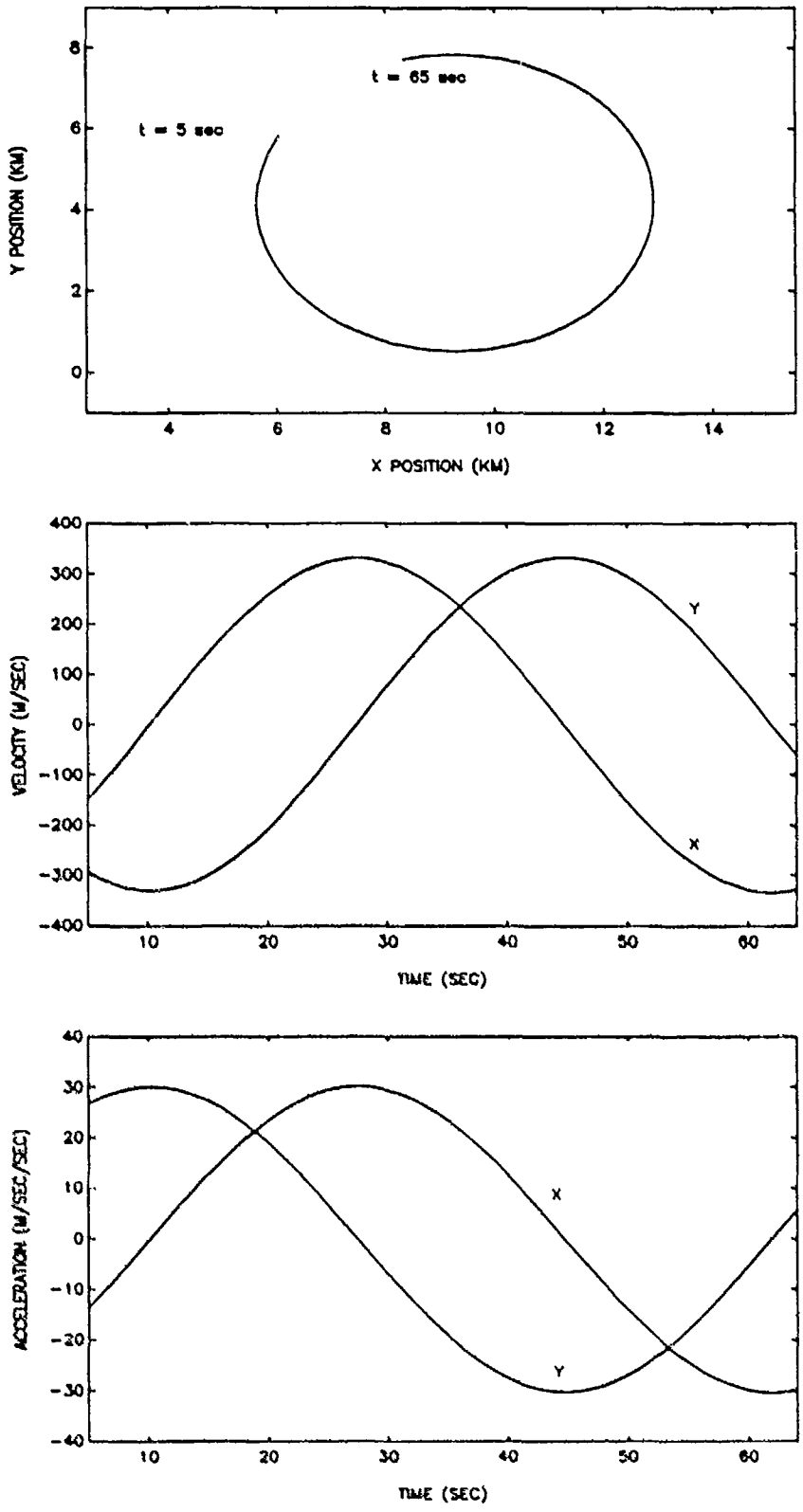

Figure 5.1 Profile of Trajectory 1

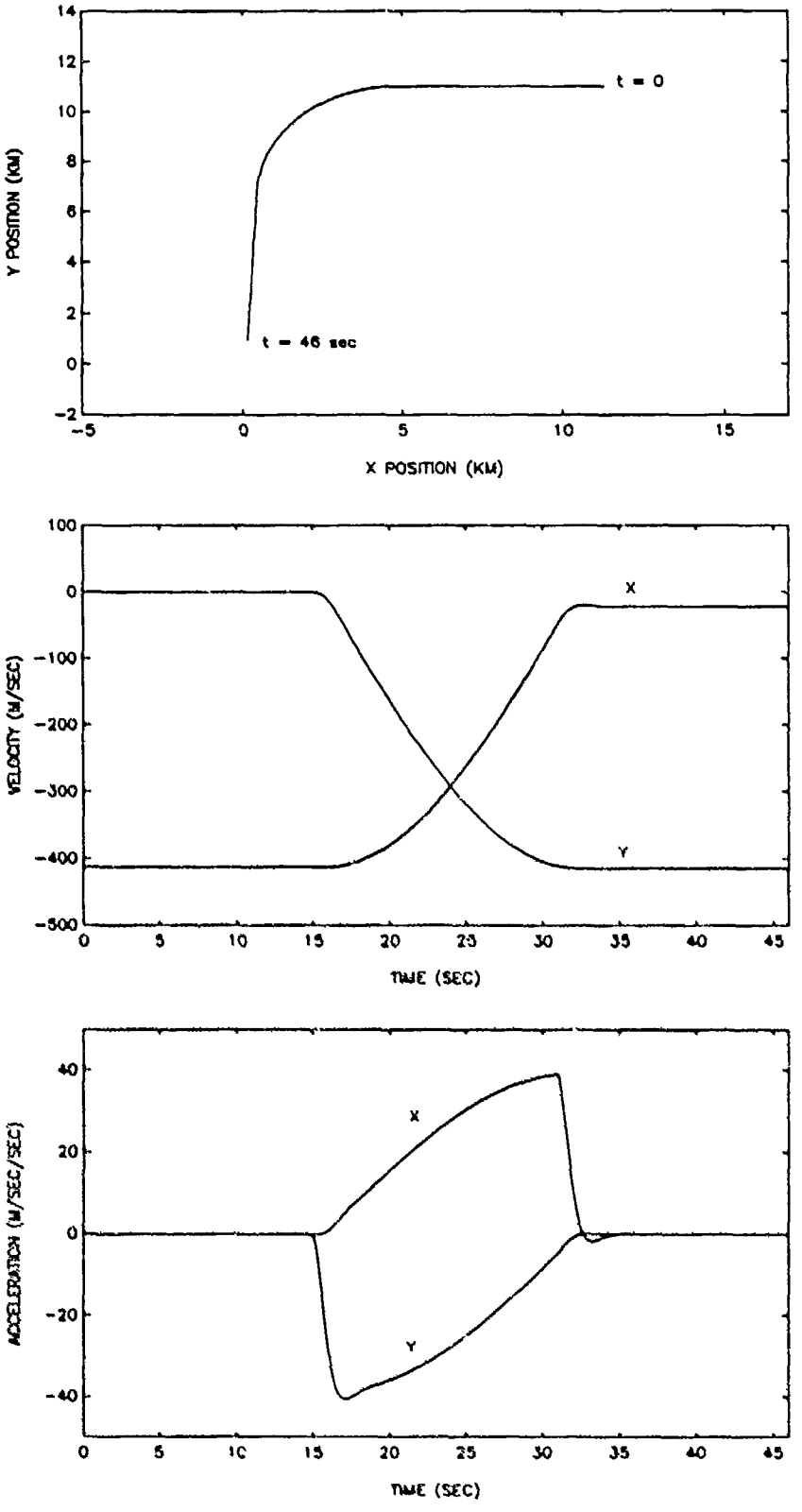

Figure 5.2 Profile of Trajectory 2

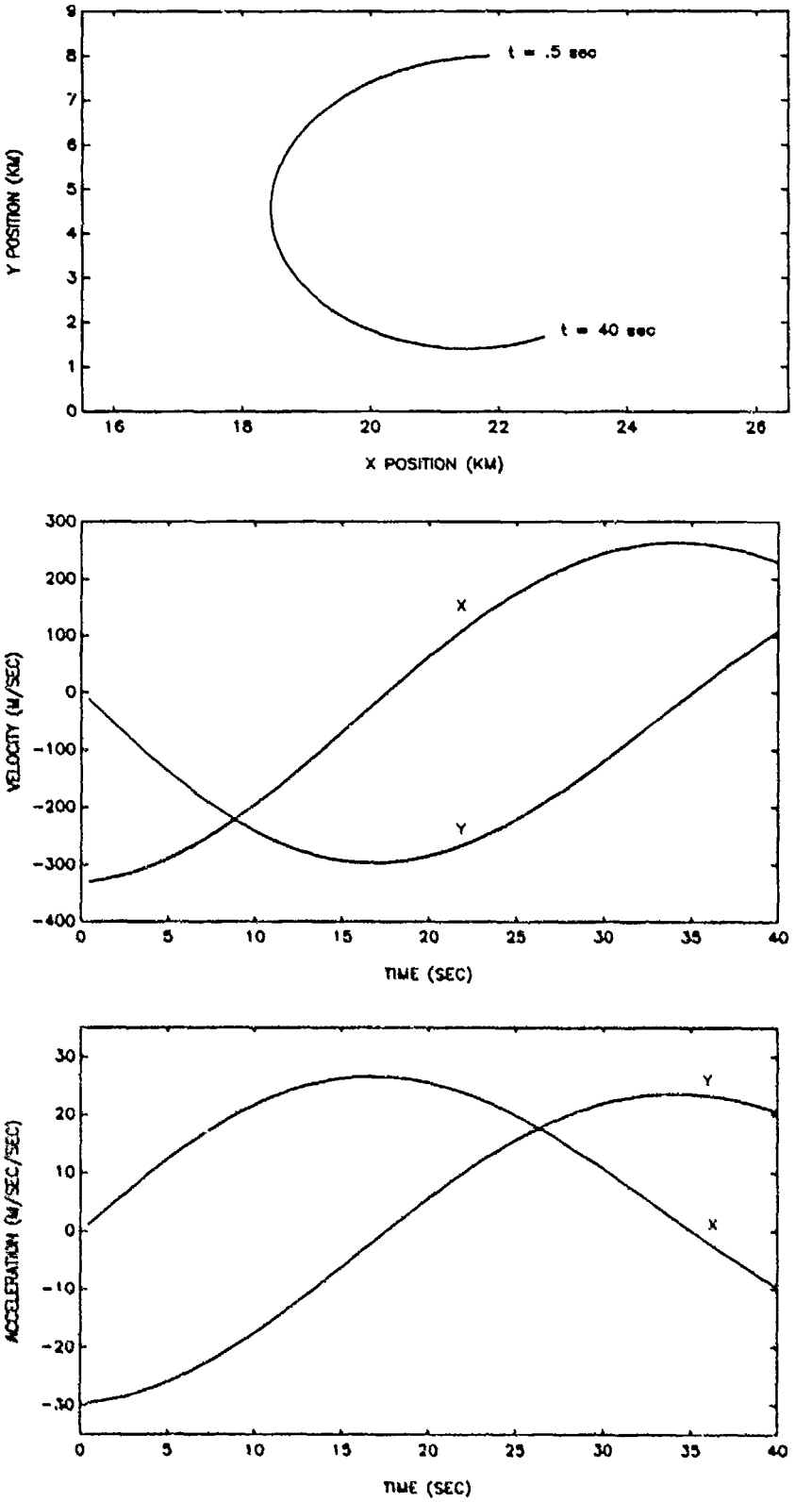

Figure 5.3 Profile of Trajectory 3

the accuracy of the filters. The parameters r_1 and δ for implementing the constraint were fixed with $r_1 = 200$ and $\delta = .9$ throughout the simulation study. The parameter γ will be adjusted to manipulate R_k^μ by its steady state value r_0.

First, simulation results will be presented to demonstrate the improvement in tracking performance provided through the use of the kinematic constraint. For this part, the data rate is 4 Hz with $\sigma_r = 8$ m and $\sigma_b = \sigma_e = 2$ mrad. The results for tracking Trajectory 1 with a kinematically constrained and an unconstrained track filter are given in Figure 5.4. The model error was $q_k = 3$ m/sec^3 for both filters and $\gamma = 2$ for the kinematically constrained one. Notice the significant improvement in position, velocity, and acceleration estimates gained through using the kinematic constraint. More improvement is achieved during filter initialization and when the target is further from the radar where the sensor errors are greater.

The tracking results for Trajectory 2 are given in Figure 5.5. The kinematically constrained filter provides improved state estimates when compared to its unconstrained counterpart for this maneuver. By using the kinematic constraint, improved target state estimates are obtained during the maneuvering portion of the flight with improvement in tracking accuracy before and after the maneuver. The model error was $q_k = 12$ m/sec^3 for both filters and $\gamma = 8$ for the kinematically constrained filter. The greatest amount of improvement occurs for the velocity and acceleration estimates.

The accuracy of the tracking results is highly dependent on the rate at which the measurements are received with higher data rates yielding better state estimates. The effects of data rate on the performance of a track filter using the kinematic constraint is considered with simulation results for data rates of 2 Hz, 4 Hz, and 10 Hz. The measurement errors are fixed with $\sigma_r = 8$ m and $\sigma_b = \sigma_e = 2$ mrad. The model error is $q_k = 3$ m/sec^3 for both filters and $\gamma = 1$ for the constrained filter. Figures 5.6, 5.7 and 5.8 give the tracking results for Trajectory 1 at data rates of 2, 4, and 10 Hz. The kinematic constraint provides about the same level of improvement in the state estimates at each data rate.

Figures 5.9, 5.10, and 5.11 give the tracking results for Trajectory 2 at 2, 4, and 10 Hz. The motion model error is $q_k = 12$ m/sec^3 for both filters and $\gamma = 1$ for the constrained filters. At all three data rates, the constrained filter outperformed its unconstrained counterpart. Note that data rate has less of an adverse effect on the performance of a kinematically constrained filter than the unconstrained one.

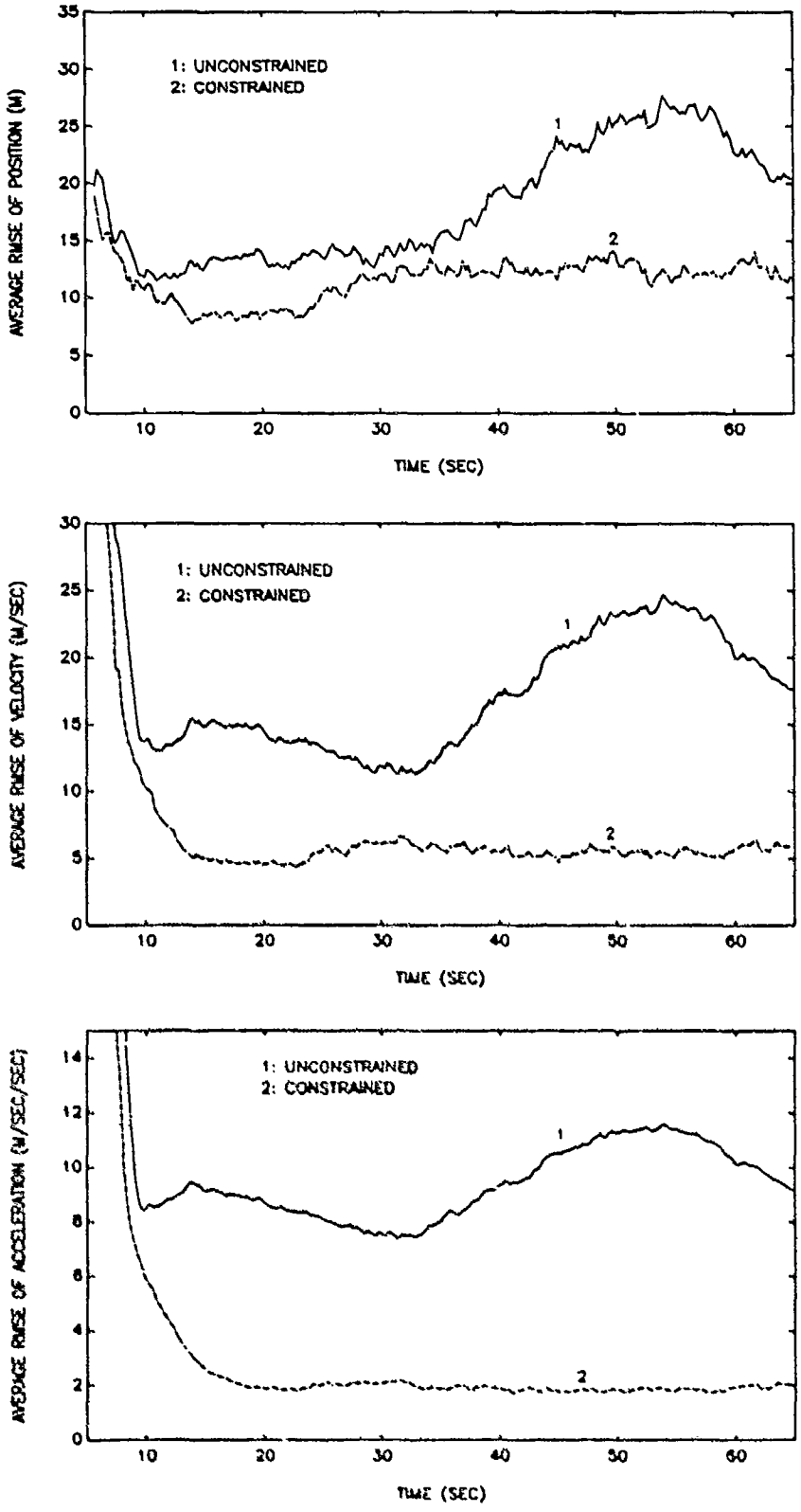

Figure 5.4 Tracking Results for Trajectory 1 With 4 Hz Data, $q_t = 3$ m/sec^3, $\gamma = 2$, $\sigma_r = 8$ m, and $\sigma_e = \sigma_b = 2$ mrad

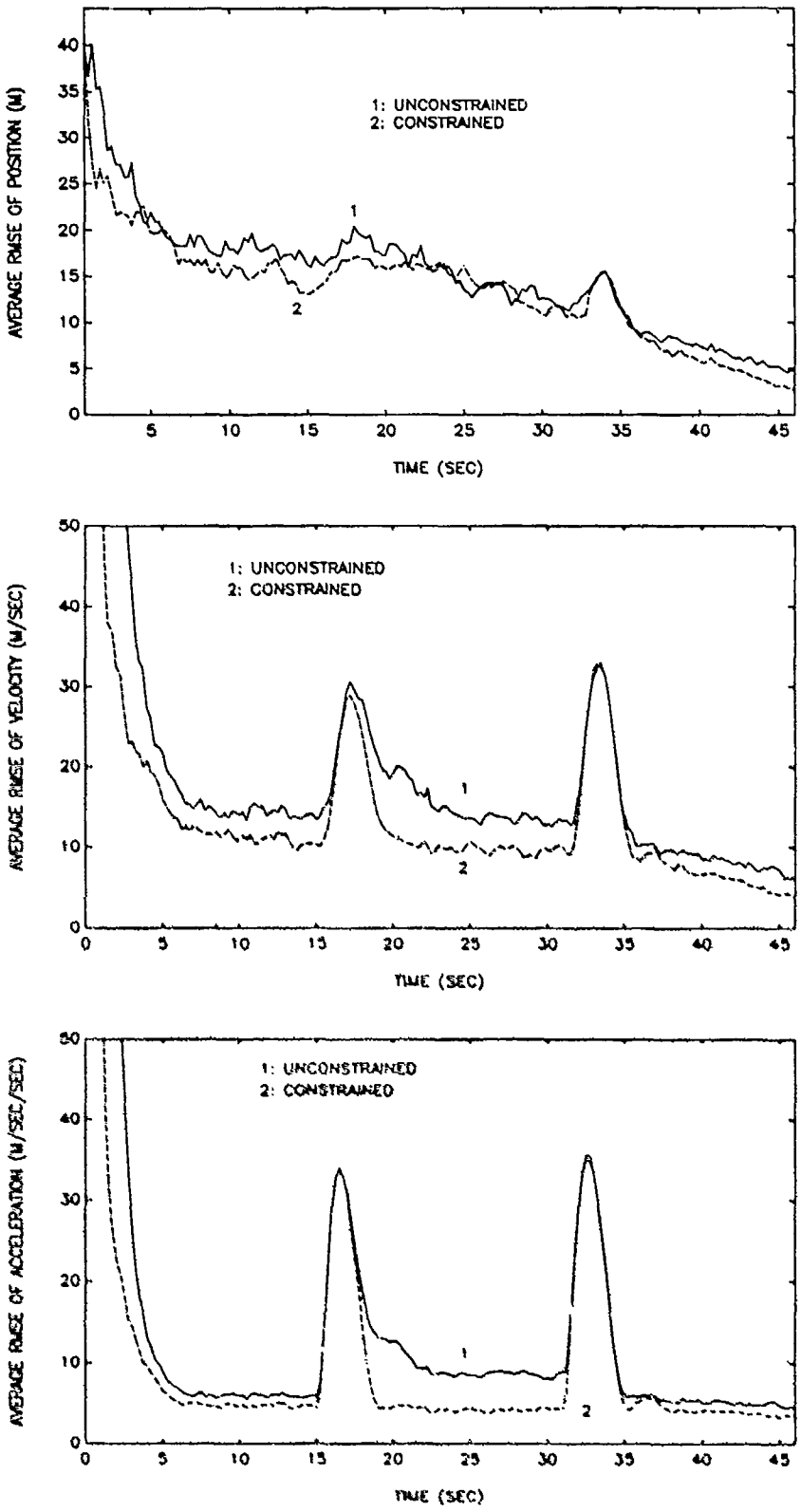

Figure 5.5 Tracking Results for Trajectory 2 With 4 Hz Data, $q_k = 12$ m/sec^3, $\gamma = 8$, $\sigma_r = 8$ m, and $\sigma_e = \sigma_b = 2$ mrad

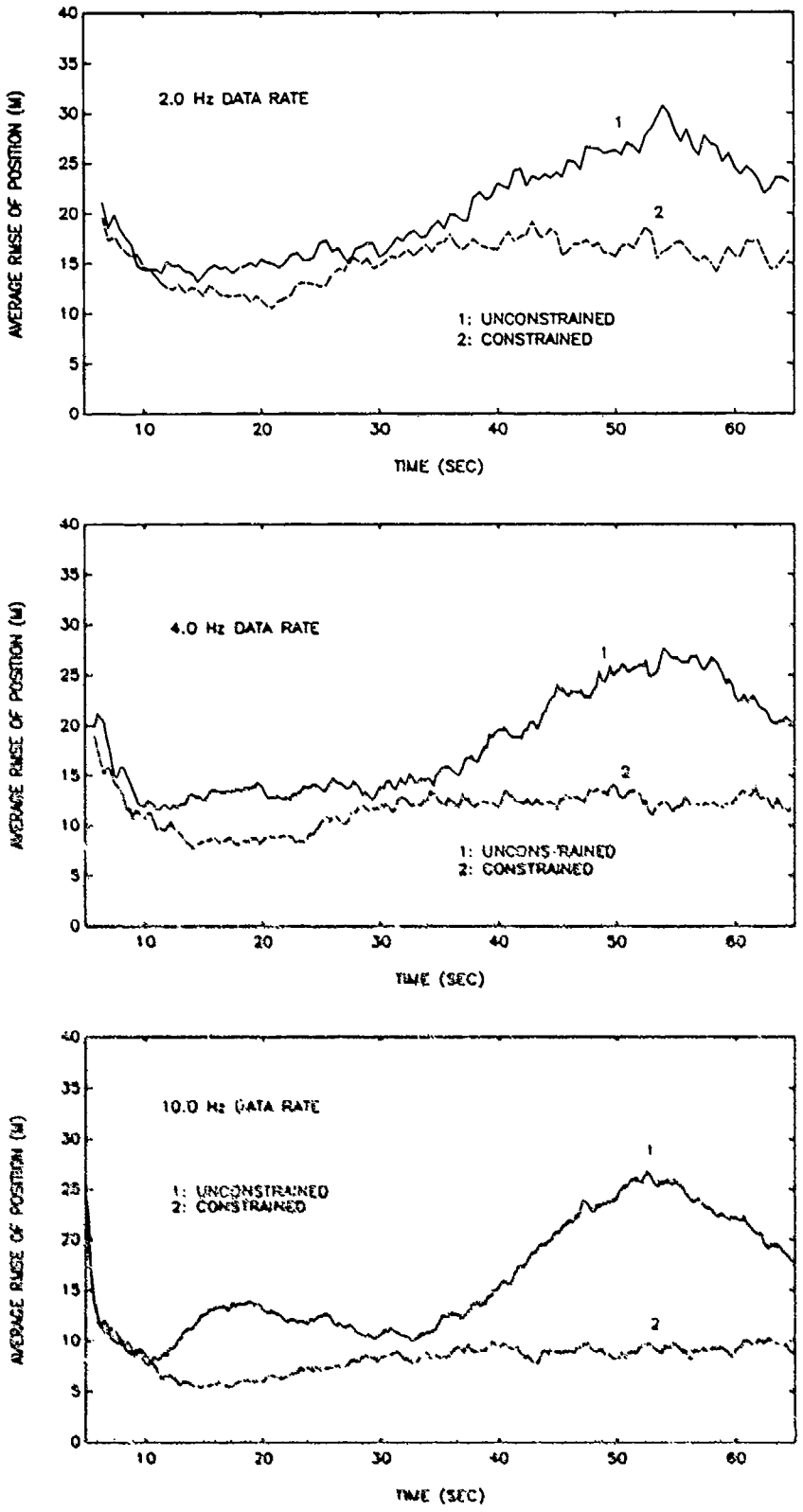

Figure 5.6 Position Error Results for Different Data Rates for Trajectory 1 With $q_k = 3$ m/sec^3, $\gamma = 1$, $\sigma_r = 8$ m, and $\sigma_\delta = \sigma_\epsilon = 2$ mrad

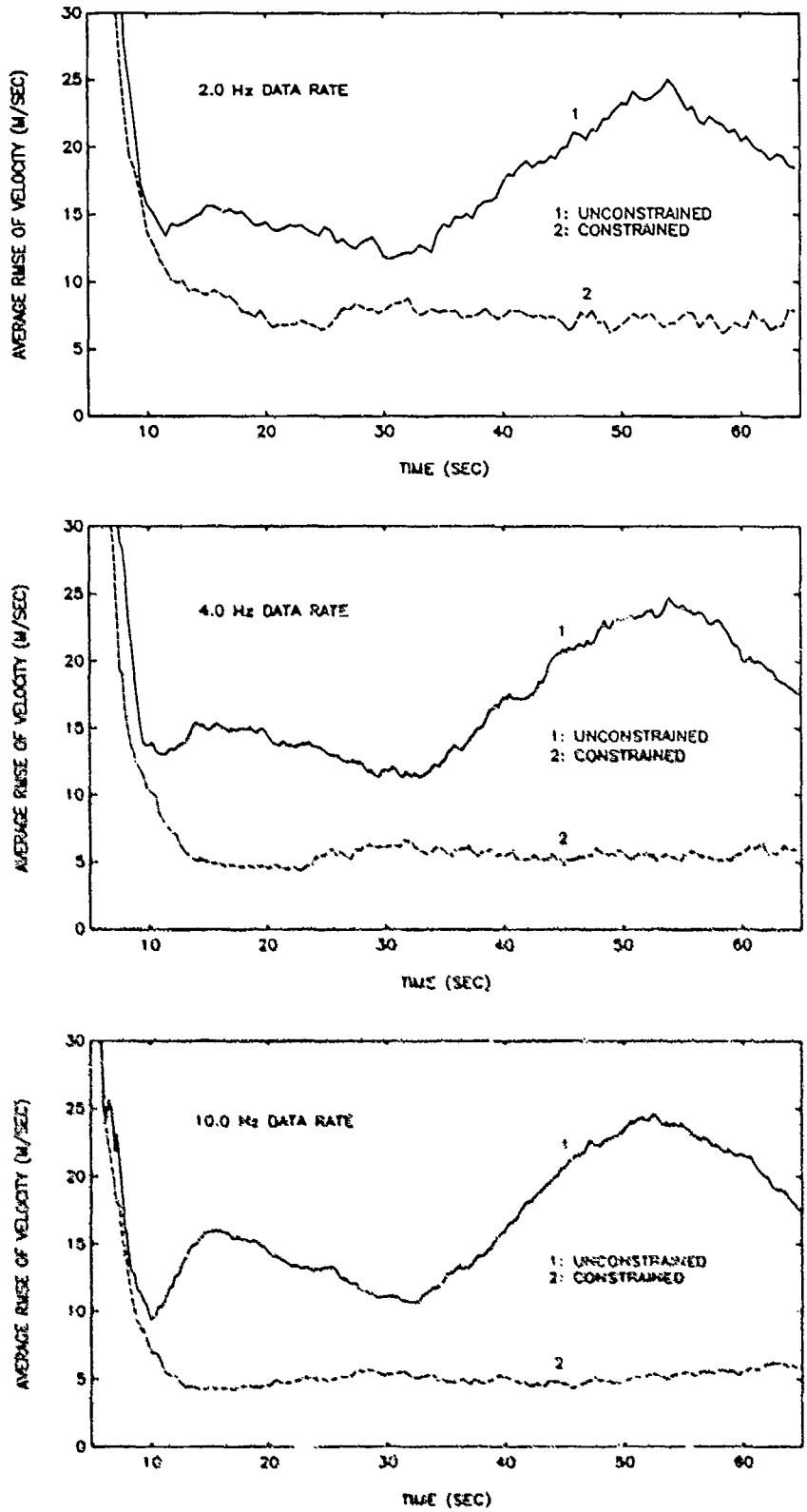

Figure 5.7 Velocity Error Results for Different Data Rates for Trajectory 1 With $q_k = 3$ m/sec^3, $\gamma = 1$, $\sigma_r = 8$ m, and $\sigma_b = \sigma_e = 2$ mrad

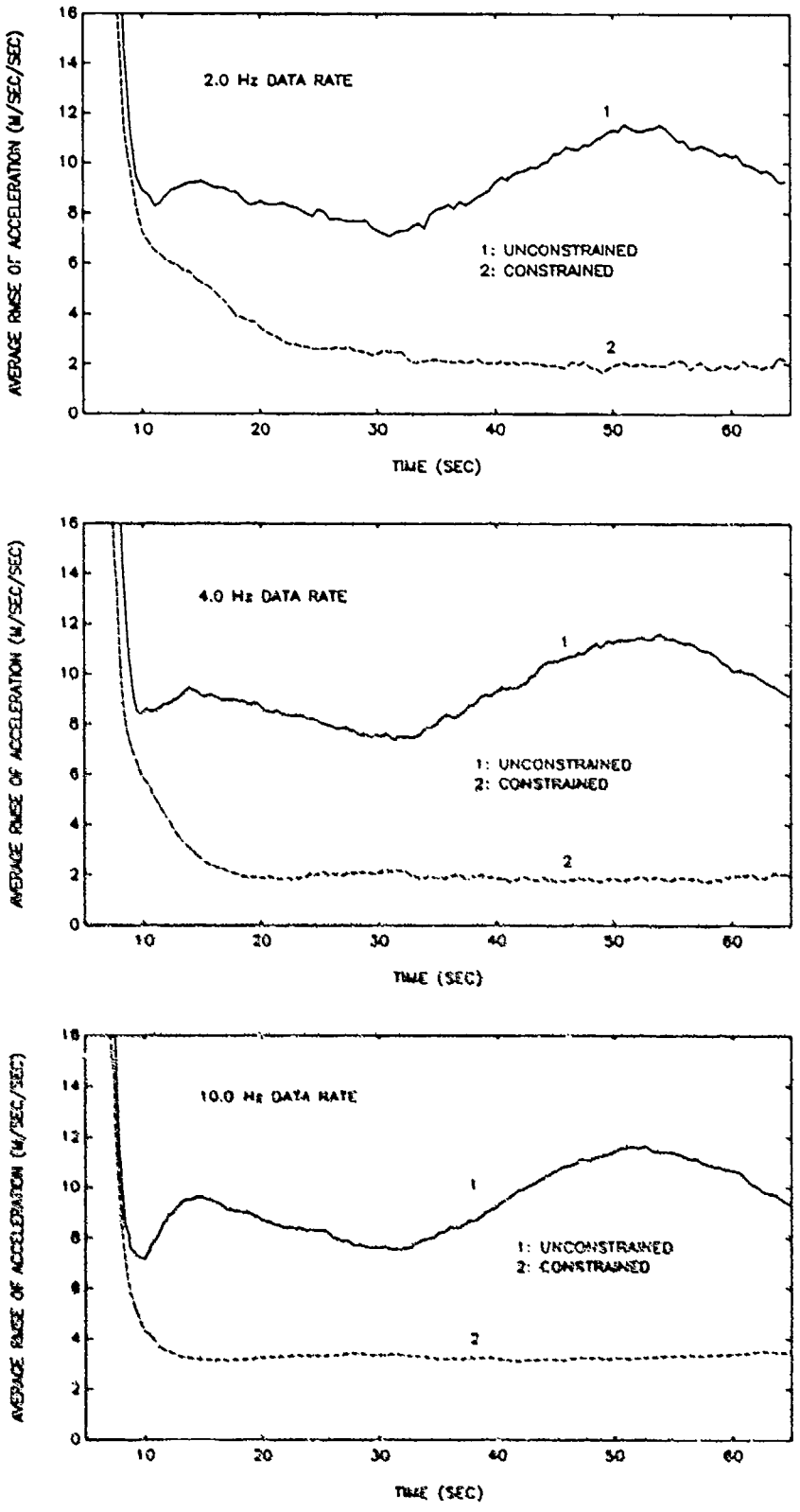

Figure 5.8 Acceleration Error Results for Different Data Rates for Trajectory 1 With $q_k = 3$ m/sec^3, $\gamma = 1$, $\sigma_r = 8$ m, and $\sigma_b = \sigma_e = 2$ mrad

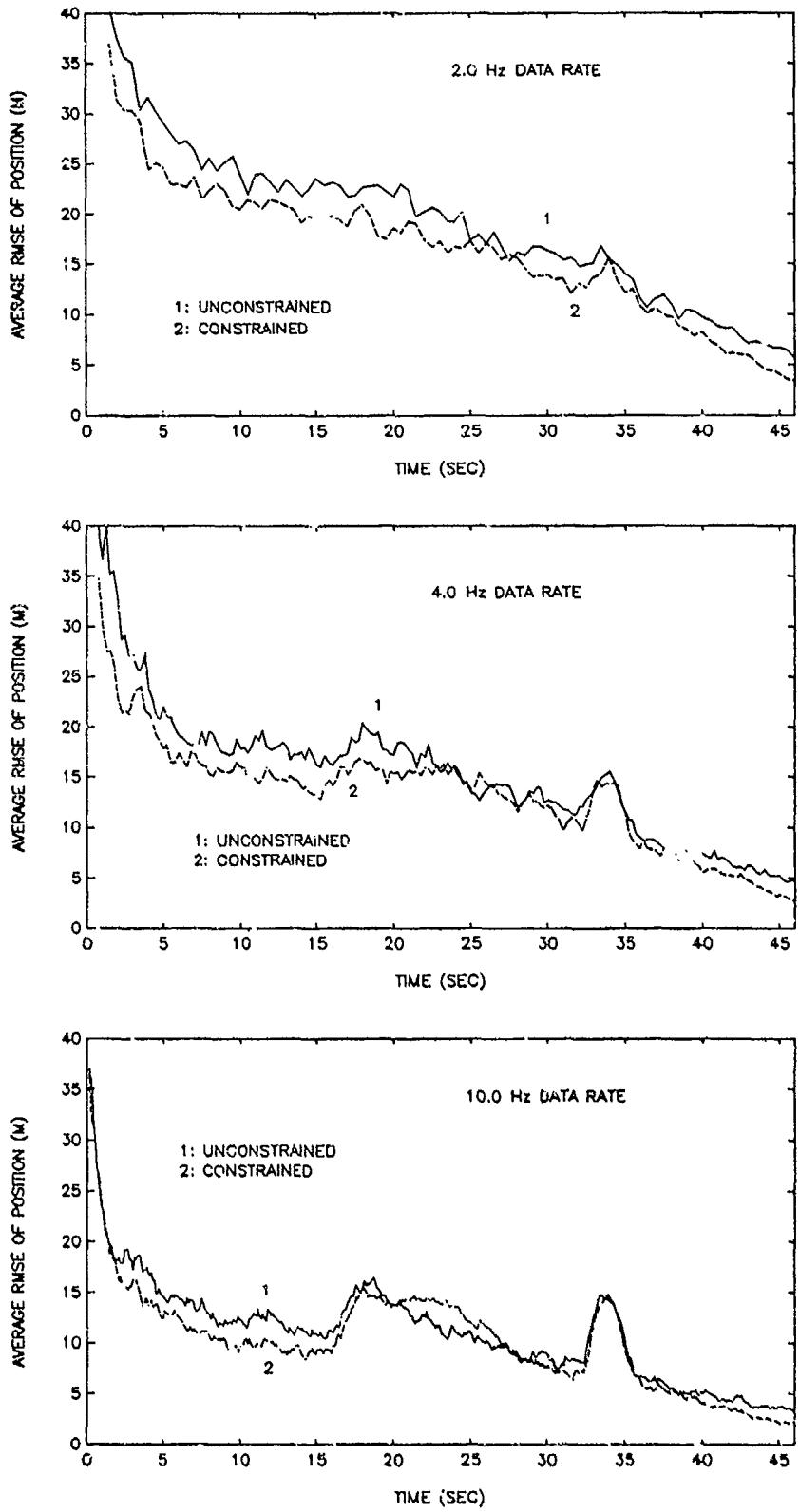

Figure 5.9 Position Error Results for Different Data Rates for Trajectory 2 With q_k = 12 m/sec^3, $\gamma = 1$, $\sigma_r = 8$ m, and $\sigma_b = \sigma_e = 2$ mrad

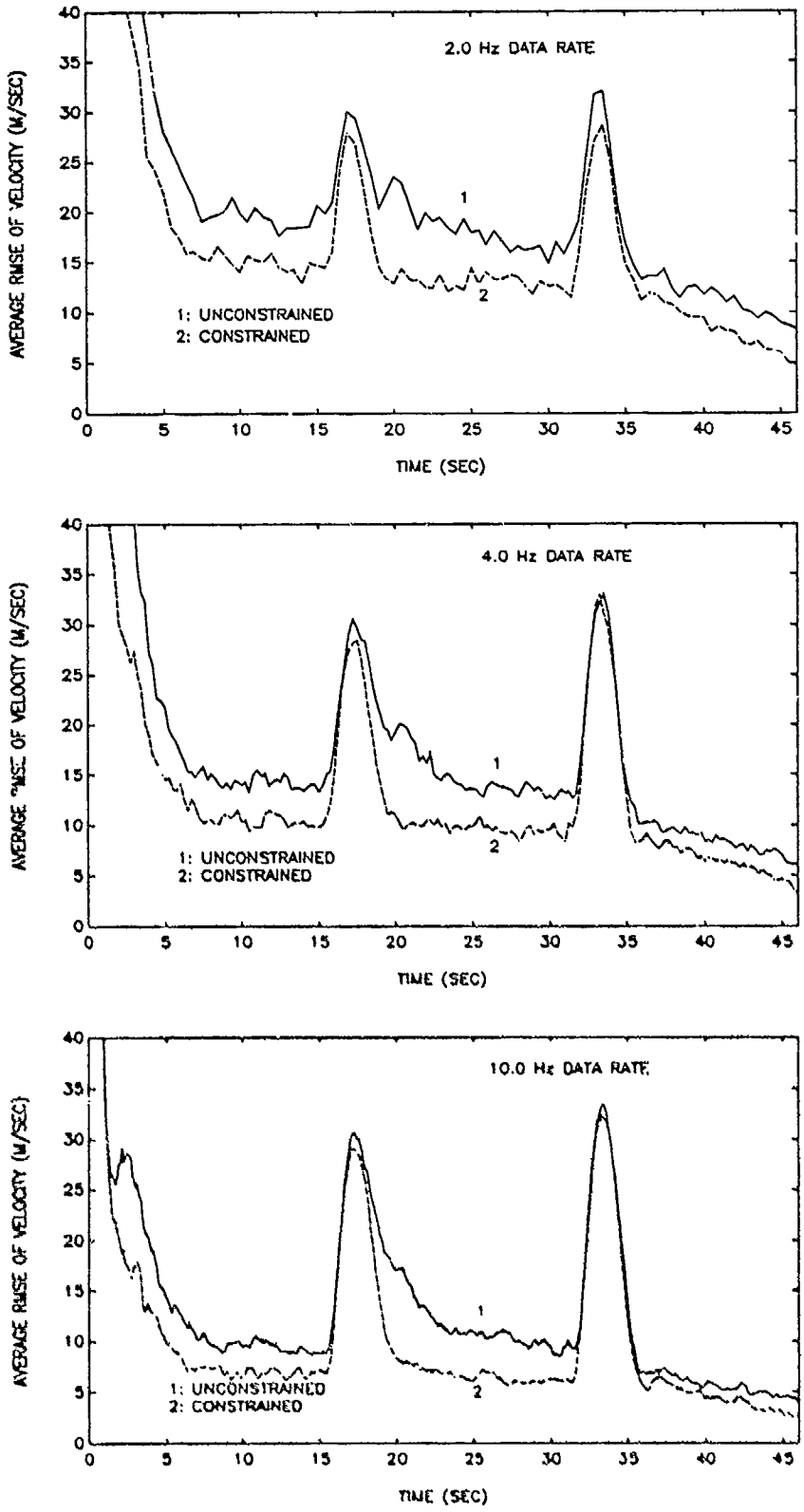

Figure 5.10 Velocity Error Results for Different Data Rates for Trajectory 2 With q_k = 12 m/sec^3, $\gamma = 1$, $\sigma_r = 8$ m, and $\sigma_b = \sigma_e = 2$ mrad

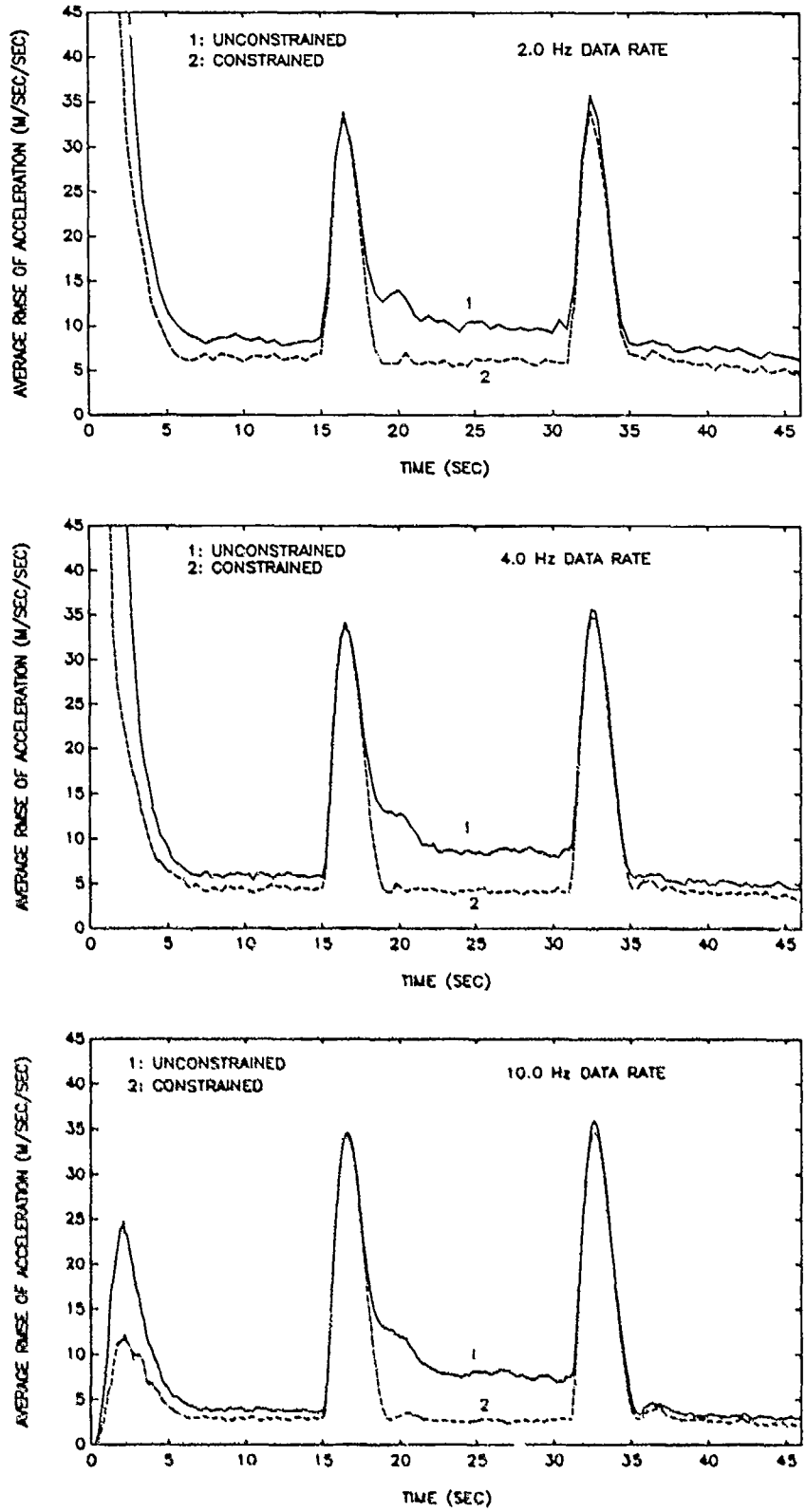

Figure 5.11 Acceleration Error Results for Different Data Rates for Trajectory 2 With $q_k = 12$ m/sec^3, $\gamma = 1$, $\sigma_r = 8$ m, and $\sigma_b = \sigma_e = 2$ mrad

The kinematically constrained track filters outperformed their unconstrained counterparts for each of the data rates considered. The tracking performance has not been maximized, but the value of the kinematic constraint is clearly demonstrated. The use of the kinematic constraint in a filter which receives its data at a low rate can track as accurate and sometimes more accurate than an unconstrained filter receiving data at a much faster rate. If a system is limited in its data rate due to hardware or other restrictions, the kinematic constraint can improve the accuracy of the state estimates of the target. Improvement in tracking accuracy for the constrained filters when compared to the unconstrained filters occurred at all the data rates considered in this part.

The effects of the constraint variance on tracking performance is of considerable importance for filter design. Steady-state variance of the constraint error is examined because the variance at initialization can be made to decay very quickly with the formulation of R_k^{μ} as given in Eq. (3.20). The effects of the constraint variance on tracking performance will be analyzed by varying γ in the formulation of r_0 given in Eq. (5.19). The effects of γ are assessed for Trajectories 1 and 2 being considered at data rates of 4 Hz and 10 Hz with $\sigma_r = 8$ m and $\sigma_e = \sigma_b = 2$ mrad. As shown in Figures 5.12 and 5.13, the effects of the constraint variance on the tracking results for Trajectory 1 were small for a data rate of 4 Hz with $\gamma = 0.5, 1, 8$ and $q_k = 3$ m/sec^3. The RMSE in position, velocity, and acceleration estimates are fairly similar for each value of γ. A slight degradation in acceleration estimates can be seen as γ decreased because the steady-state variance was increasing. However, this is only a small degradation in performance in this case. Decreasing the constraint variance could provide slight increases in tracking performance, but simply applying the constraint is sufficient to provide improved tracking results.

For the circular trajectory with a 10 Hz data rate and $\gamma = 0.5, 10, 20$, varying γ has a significant effect on the performance of a kinematically constrained filter. This point is shown in Figure 5.13. The steady-state constraint variance increases and becomes too loose as γ is decreased. There is a distinct separation in the accuracy of the velocity and acceleration estimates. The best performance occurred when $\gamma = 20$; slight increases in performance could occur if γ was increased to tighten the constraint variance. Notice the position and velocity estimates beginning to diverge toward the end of the maneuver when $\gamma = 0.5$ and the data rate is at 10 Hz. This is again a result of setting the constraint variance too large.

The effects of the constraint variance are considered for the target making a 90 degree turn. The model error is again $q_k = 12$ m/sec^3, with $\gamma = 1/16, 8$. The results for a 4 Hz data rate are shown in Figure 5.14. Changing the value of the steady state constraint has

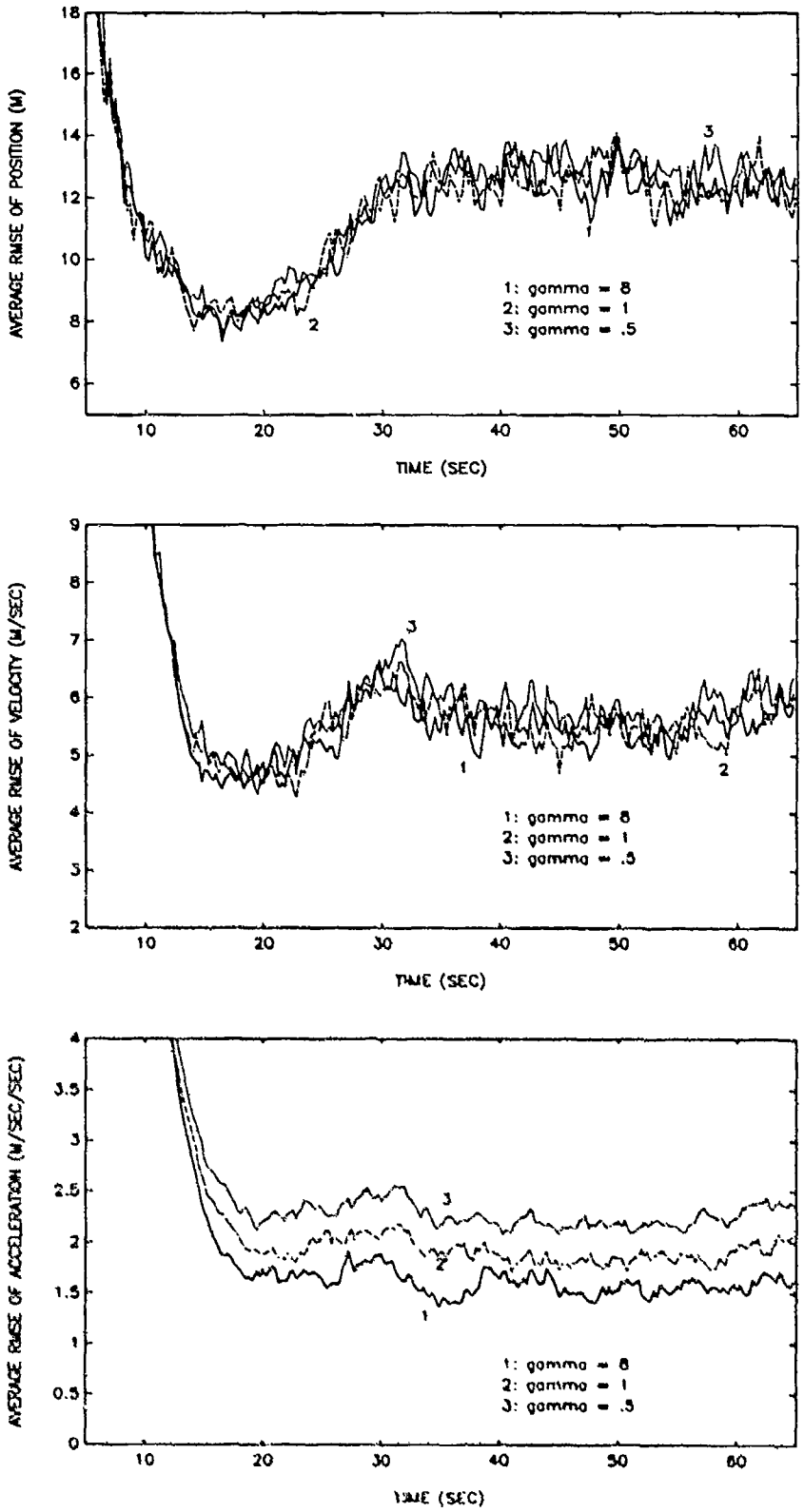

Figure 5.12 Results for Different Constaint Variances for Trajectory 1 With 4 Hz Data, $q = 3$ m/sec^3, $\sigma_r = 8$ m, and $\sigma_e = \sigma_b = 2$ mrad

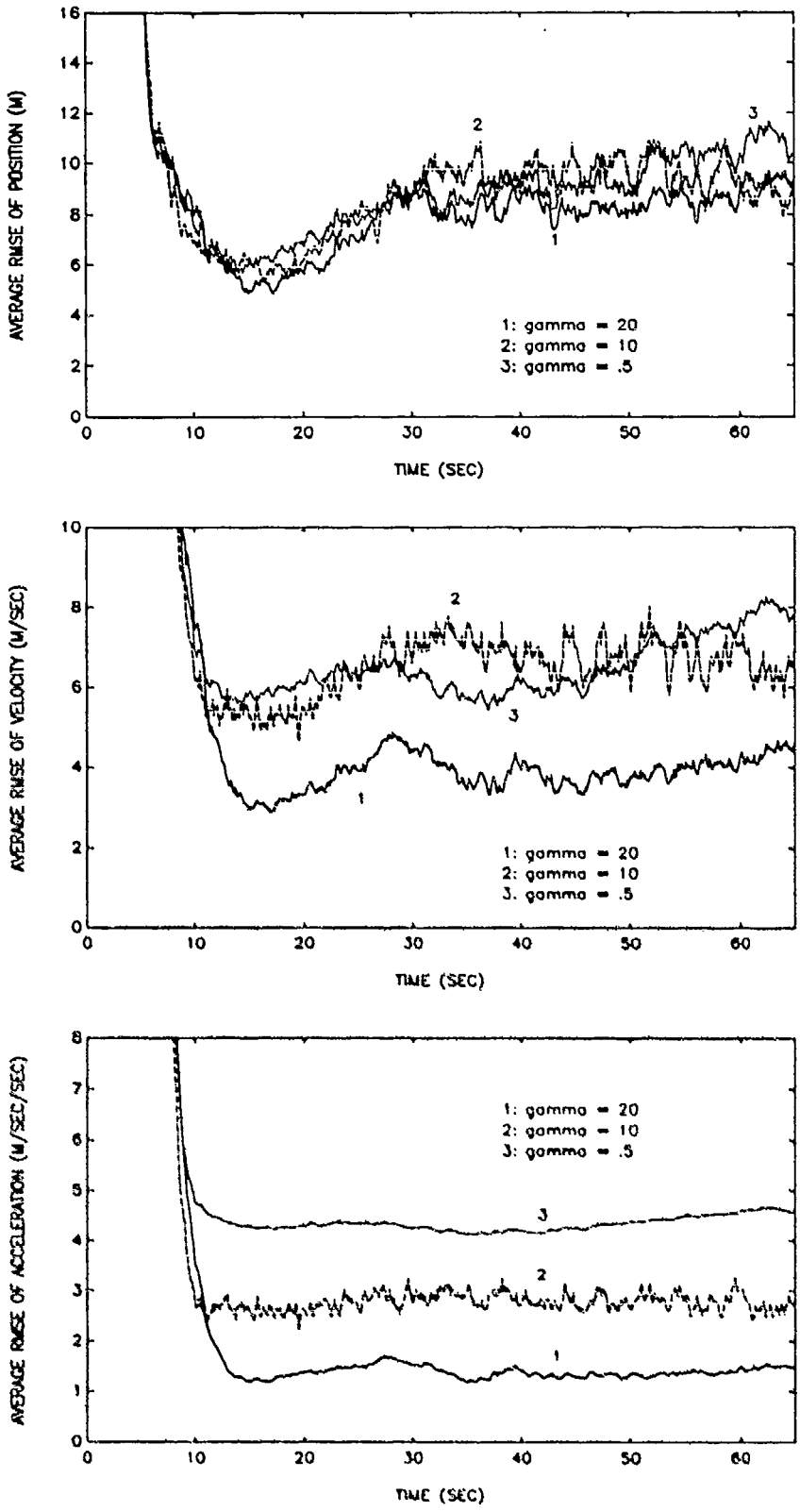

Figure 5.13 Results for Different Constaint Variances for Trajectory 1 With 10 Hz Data, $q = 3$ m/sec^3, $\sigma_r = 8$ m, and $\sigma_\epsilon = \sigma_b = 2$ mrad

very little effect on the overall performance of the track filter. The position and velocity estimates are quite similar for each value of γ with a slight difference in results occurring for the position estimates. Decreasing γ loosened the constraint variance and improved the tracking of the position. The tracking performance is essentially insensitive to the constraint variance in this case. However, the position estimates from the kinematically constrained filters are highly sensitive to the constraint variance for a data rate of 10 Hz. In Figure 5.15, the position estimates improved as the constraint variance was loosened by decreasing γ. There are also slight changes in the velocity results, but the changes are not obvious due to the amount of error incurred at the beginning and end of the turn.

The steady-state constraint variance can be very critical to the tracking accuracy of a kinematically constrained filter. If the target is in a maneuver, the variance should be tightened by increasing γ in order to track the target more accurately. However, if the target is going through a complete maneuver, the constraint should be applied very loosely by decreasing γ to attain greater accuracy. Increasing the variance allows the kinematic constraint to track a wider range of maneuvers more accurately. It is important to know the data rate and model error when choosing γ. An improper choice of γ may not provide the most accurate results. The constraint variance should be based on the data rate and model error so that tracking improvement can occur for the maneuver with the largest change in acceleration.

The effects of measurement error on the performance of the kinematic constraint are discussed next. The two trajectories have three different amounts of measurement error added to them to simulate different sensor accuracies. The three noise levels are denoted as low, medium, and high. Low noise has $\sigma_r = 4$ m and $\sigma_\epsilon = \sigma_b = 1$ mrad, medium noise has $\sigma_r = 8$ m and $\sigma_\epsilon = \sigma_b = 2$ mrad, and high noise has $\sigma_r = 12$ m and $\sigma_\epsilon = \sigma_b = 3$ mrad. The filters operate at a 4 Hz data rate with $\gamma = 1$ for the constrained filters. A comparison is made between the kinematically constrained and unconstrained track filters for each noise level.

The effects of measurement error on tracking performance for the target performing a circular maneuver are presented first. The tracking results of the unconstrained filter are highly dependent on the amount of measurement and process error as shown in Figure 5.16. As expected, the accuracy of the state estimates increases as the amount of error decreases. The results for the constrained filters are shown in Figure 5.17. The tracking accuracy for the constrained filters at the different noise levels is much better than the unconstrained filters. The acceleration tracking accuracy for the constrained filters is somewhat insensitive

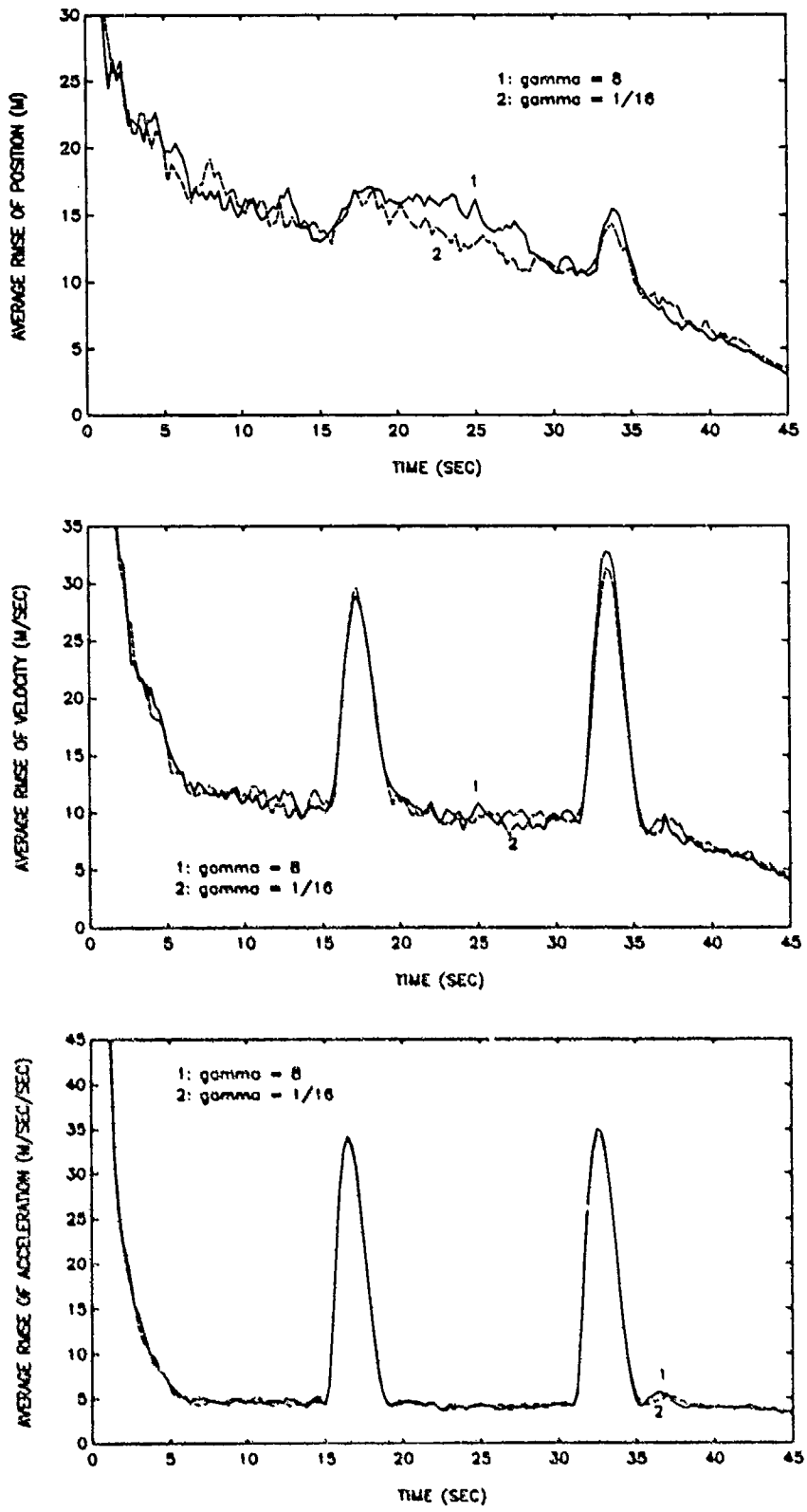

Figure 5.14 Effects of Constraint Variance for Trajectory 2 With 4 Hz Data, $q_k = 12$ m/sec^3, $\sigma_r = 8$ m, and $\sigma_\epsilon = \sigma_b = 2$ mrad

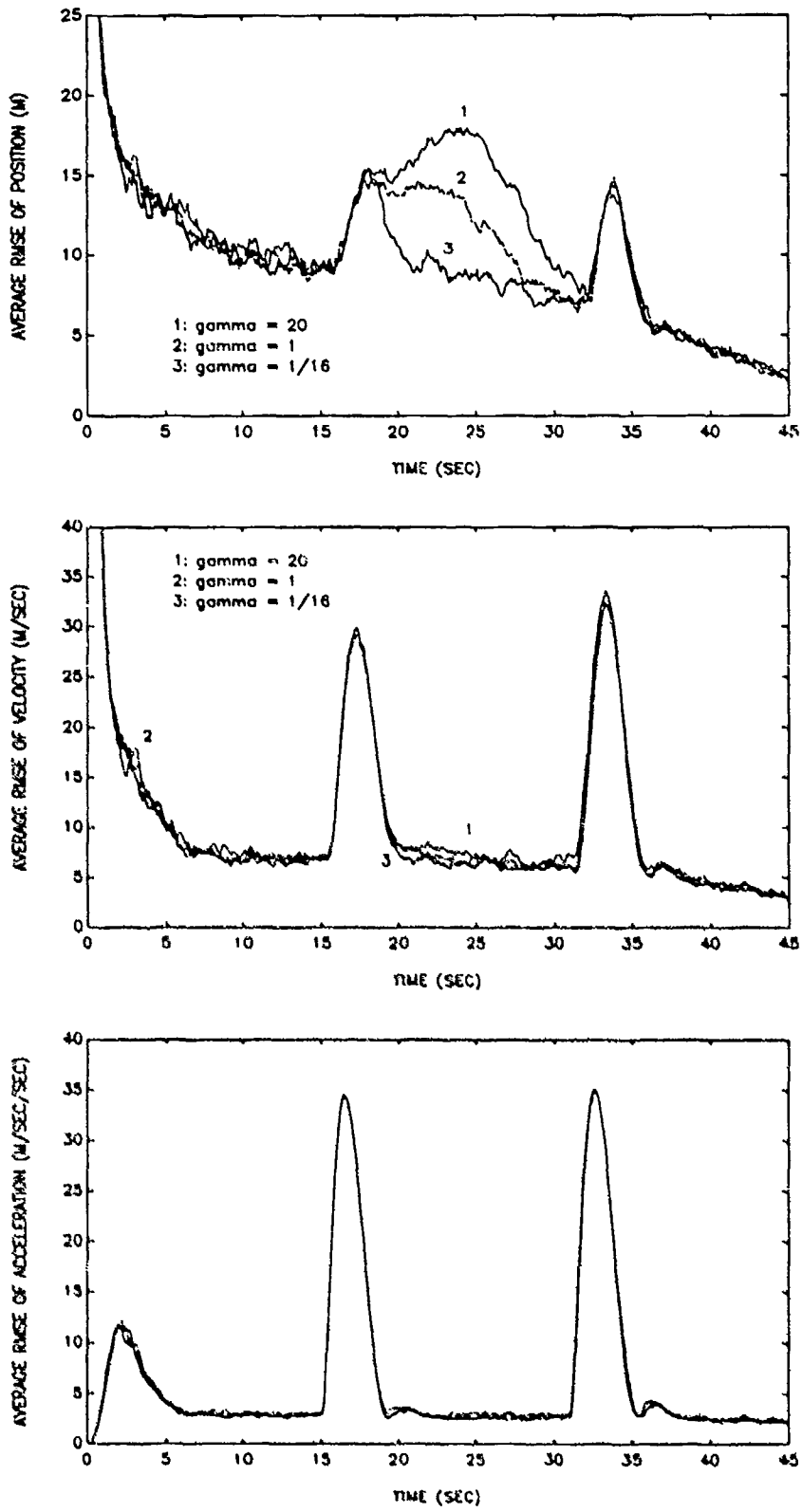

Figure 5.15 Effects of Constraint Variance for Trajectory 2 With 10 Hz Data, $q_k = 12$ m/sec^3, $\sigma_r = 8$ m, and $\sigma_\epsilon = \sigma_b = 2$ mrad

to the size of σ_r, σ_δ, and σ_ϵ for this maneuver. The velocity tracking accuracy is slightly sensitive with the most sensitivity shown in the position estimates. The constrained track filters are less sensitive to the amount of measurement noise than the unconstrained filters for this circular maneuver.

The effect measurement error has on tracking accuracy for the 90 degree turning target is not as obvious as the target maneuvering in a circle. Both types of filters appear to provide the same tracking estimates. The unconstrained filter results are shown in Figure 5.18. As expected, an increase in tracker accuracy occurs when the error decreases, with the most improvement in the position and velocity states. When compared to its constrained counterparts as in Figure 5.19, most of the improvement using the kinematically constrained filter occurs in the maneuver portion of the target trajectory. The kinematically constrained filters did provide better state estimates than their unconstrained counterparts for the different noise levels used in the study.

This part of the simulation results is devoted to deviations in target speed. The previous parts involve tracking targets maneuvering at constant speed. The kinematic constraint is designed to track this type of maneuver. However, if the target deviates from constant speed, can the kinematically constrained track filter provide better results than an unconstrained one? What must be done to ensure that the tracking is accurate throughout the maneuver? This is the focus of the following simulation results.

Trajectory 3 includes a maneuver with a deviation in speed. The target has a constant height of 200 m and is making a circular-type maneuver. The duration of the turn is 40 sec and has an initial and final speeds of 330 m/sec and 250 m/sec, respectfully. The total acceleration also changes from an initial magnitude of 3 g to 2.3 g. As a result, the general trend of the target is to spiral in on itself. There are two sets of simulation results for this part. The first set has a data rate of 4 Hz and the second a data rate of 10 Hz, but both have a model error of $q_k = 3$ m/sec^3 and measurements errors of $\sigma_r = 8$ m and $\sigma_\epsilon = \sigma_\delta = 2$ mrad. The kinematically constrained filters are compared to their unconstrained counterparts. Various values of γ were used to tighten or loosen the constraint variance.

The tracking results for the 4 Hz data rate shown in Figure 5.20 indicate that the kinematic constraint can be employed to improve the estimation accuracy even if the target does not maintain constant speed. The constraint variance must be very loose throughout the entire maneuver for improvement in tracking to be maintained. When γ is set to large, the state estimates eventually degrade to a point where the unconstrained filter outperforms the

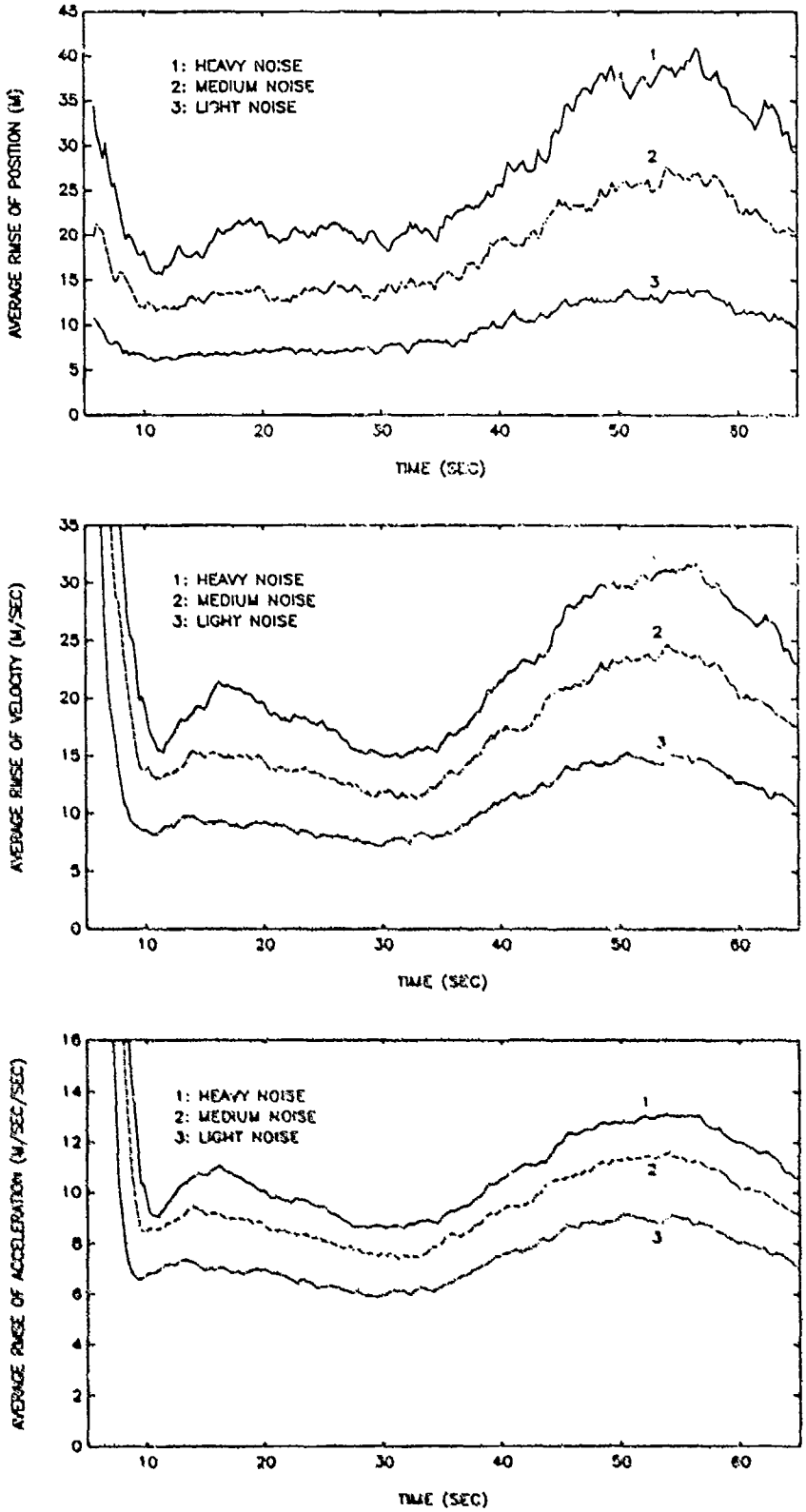

Figure 5.16 Effects of Measurement Errors on Unconstrained Filters for Tracking Trajectory 1 With 4 Hz Data, $q_t = 3$ m/sec^3, and $\gamma = 1$

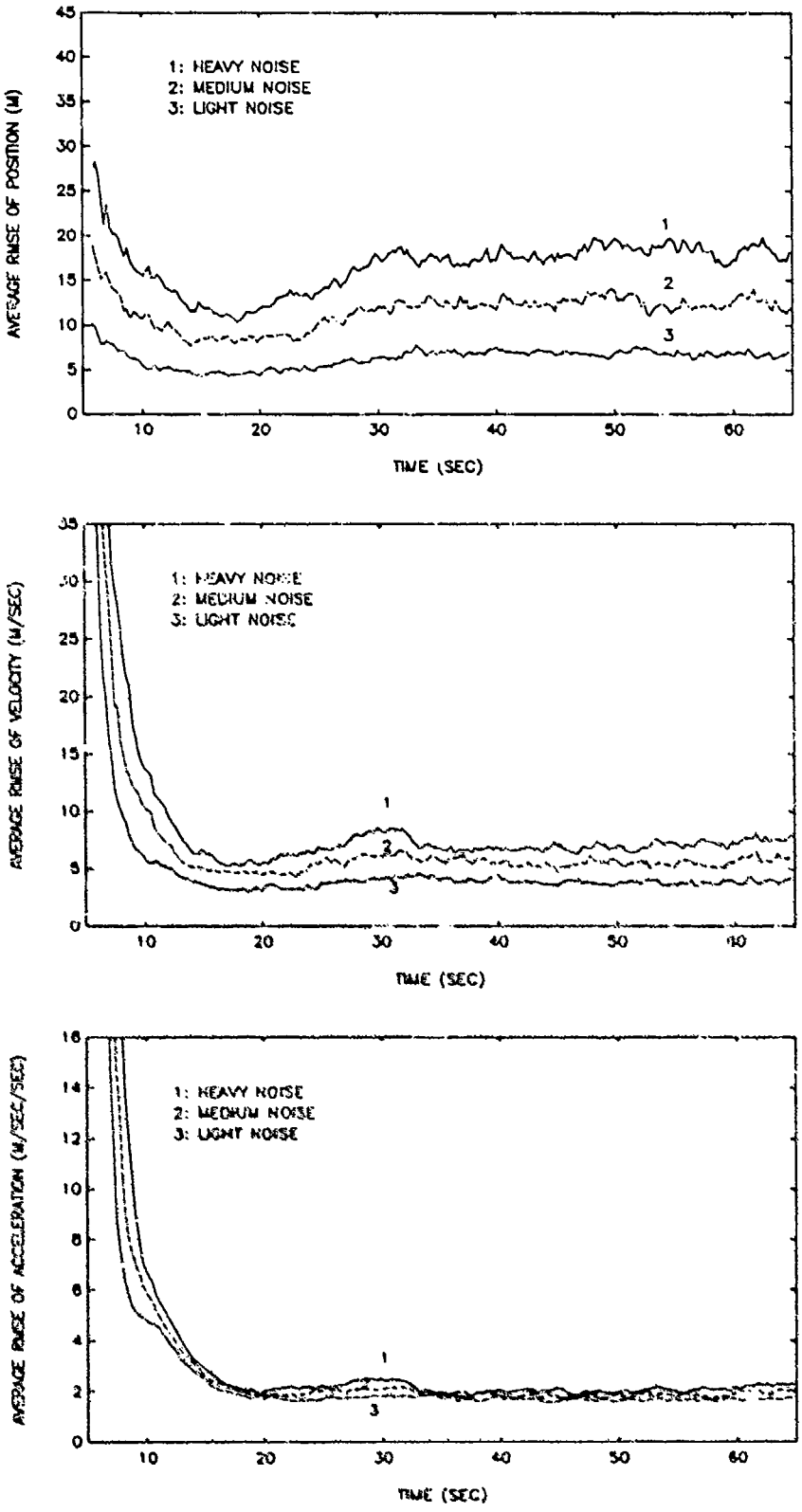

Figure 5.17 Effects of Measurement Errors on Constrained Filters for Tracking Trajectory 1 With 4 Hz Data, $q_k = 3$ m/sec^3, and $\gamma = 1$

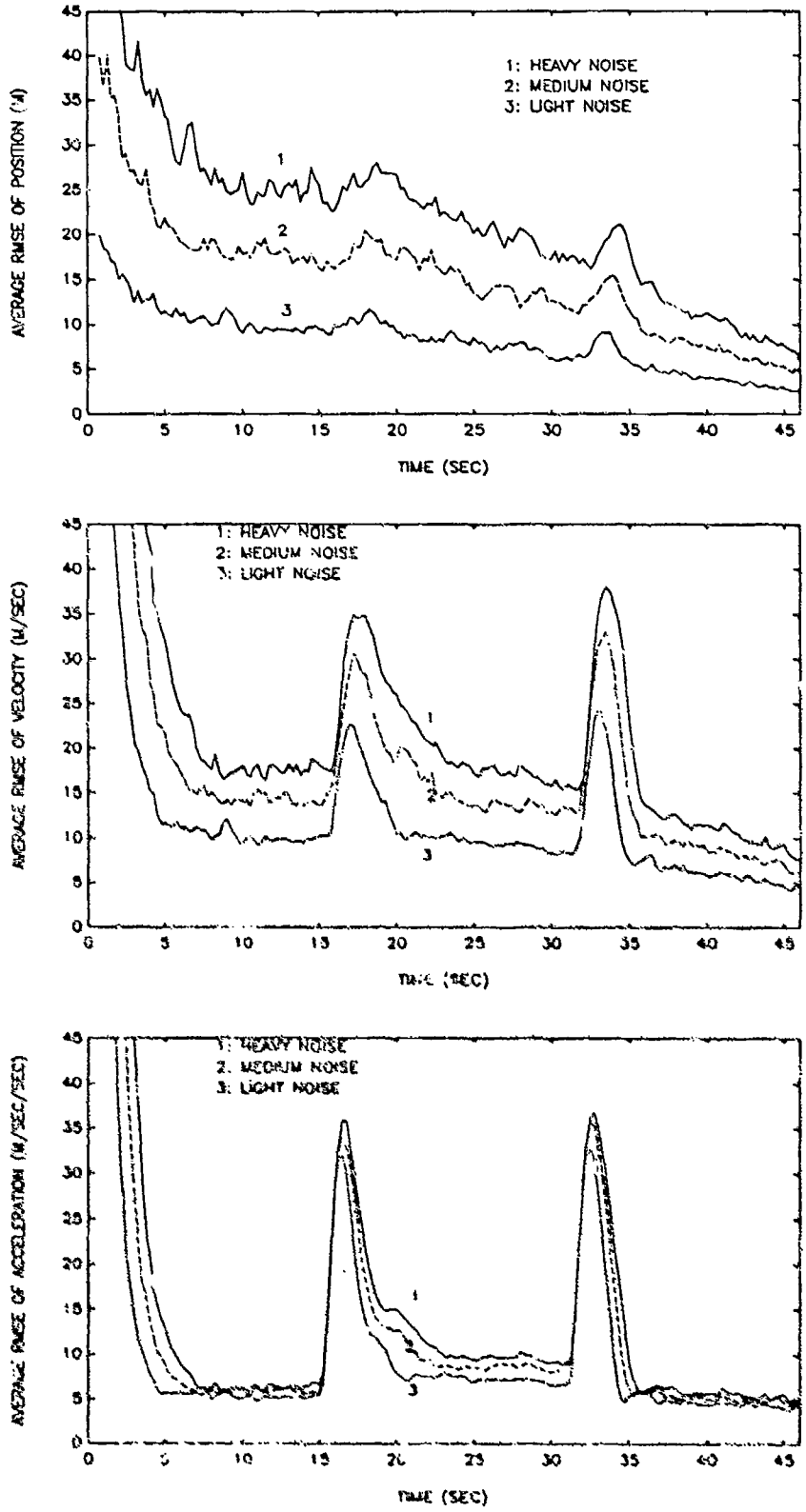

Figure 5.18 Effects of Measurement Errors on Unconstrained Filters Tracking Trajectory 2 With 4 Hz Data, $q_k = 12$ m/sec^3, and $\gamma = 1$

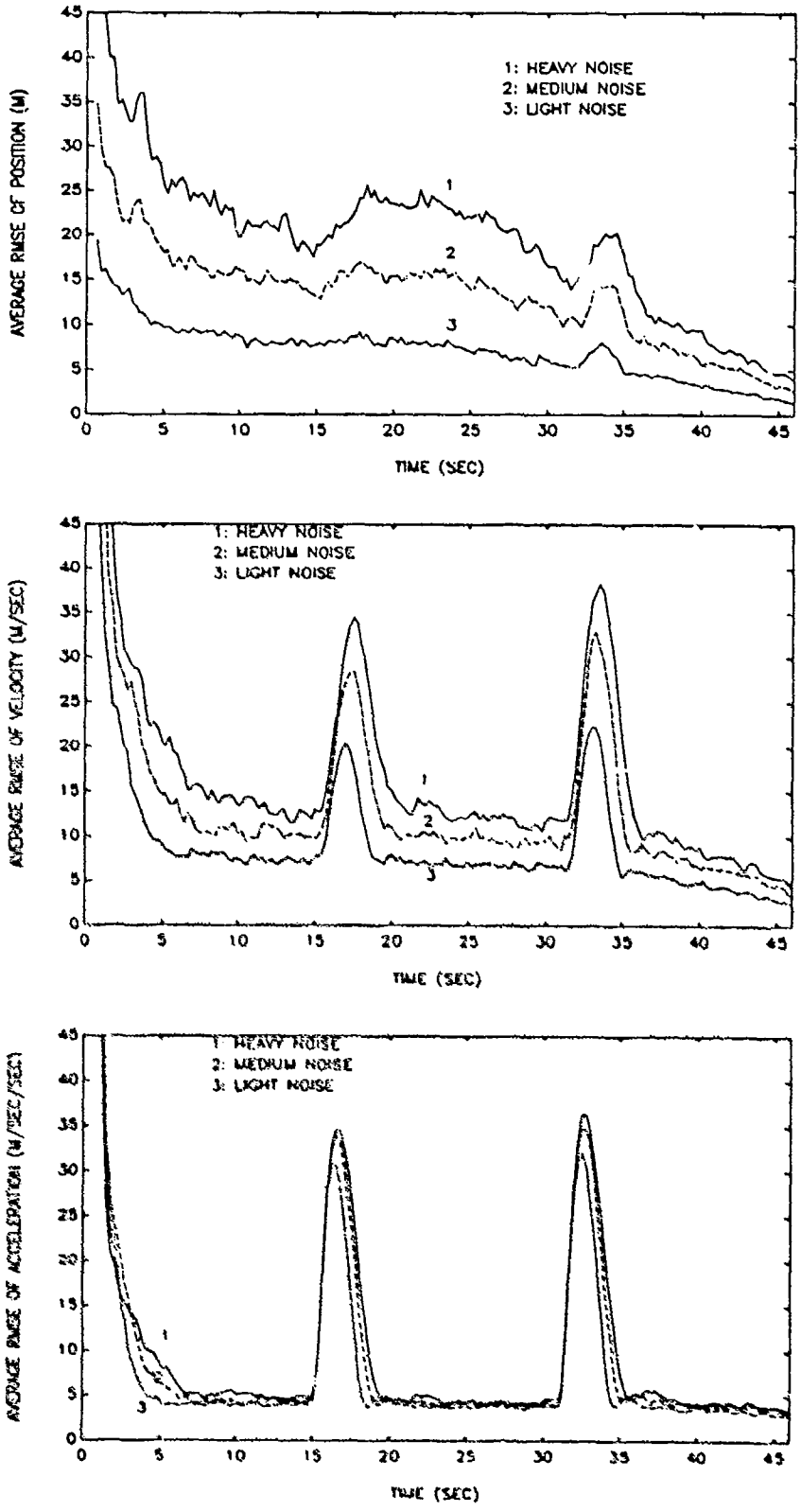

Figure 5.19 Effects of Measurement Errors on Constrained Filters Tracking Trajectory 2 With 4 Hz Data, $q_k = 12$ m/sec^3, and $\gamma = 1$

constrained one. This is highly evident in the position and velocity estimate results. However, when the constraint variance is set loosely, improved state estimates can be achieved through the entire maneuver.

The tracking results for 10 Hz are very similar to the 4 Hz data rate results. As shown in Figure 5.21, the constraint must be set extremely loose for improvement to occur throughout the entire duration of the maneuver. If the constraint variance is set too tightly, the state estimates begin to diverge during the maneuver. The constraint must be applied loosely if the target is not maneuvering at constant speed. Thus, non-constant speed targets can be tracked with improved accuracy with the constant speed kinematic constraint if the constraint variance is set properly.

SUMMARY OF THE SIMULATION RESULTS

The formulation and implementation of the constant speed kinematic constraint as a pseudomeasurement can improve the tracking accuracy of maneuvering targets. The simulation results clearly demonstrate that the kinematic constraint is a useful technique to improve tracking accuracy. The effects of data rate, measurement error, and constraint variance were all investigated. For each of these variants, the kinematically constrained filter outperformed its unconstrained counterpart. The sensitivity to increases in measurement noise of the tracking results for the constrained track filters is substantially less than that of the unconstrained filters.

The performance of kinematically constrained filters can be tuned using the constraint variance. In most cases, simply applying the kinematic constraint in the track filter using an arbitrary constraint variance is enough to provide improved tracking results. However, the type of maneuver, data rate, and model error must be considered before the value of γ is chosen. An improper choice of γ can yield tracking results which do not provide the most improvement in performance. The constraint variance is a very significant parameter the user can manipulate to achieve the degree of improvement desired.

The formulation of the kinematic constraint was designed to improve tracking performance by reducing the error in the acceleration estimates of the target. The simulation results support this point. The increase in acceleration estimate accuracy provided much needed improvement of the velocity estimates. The improvement in estimating the target state, especially the velocity and acceleration, is important for weapons and fire control.

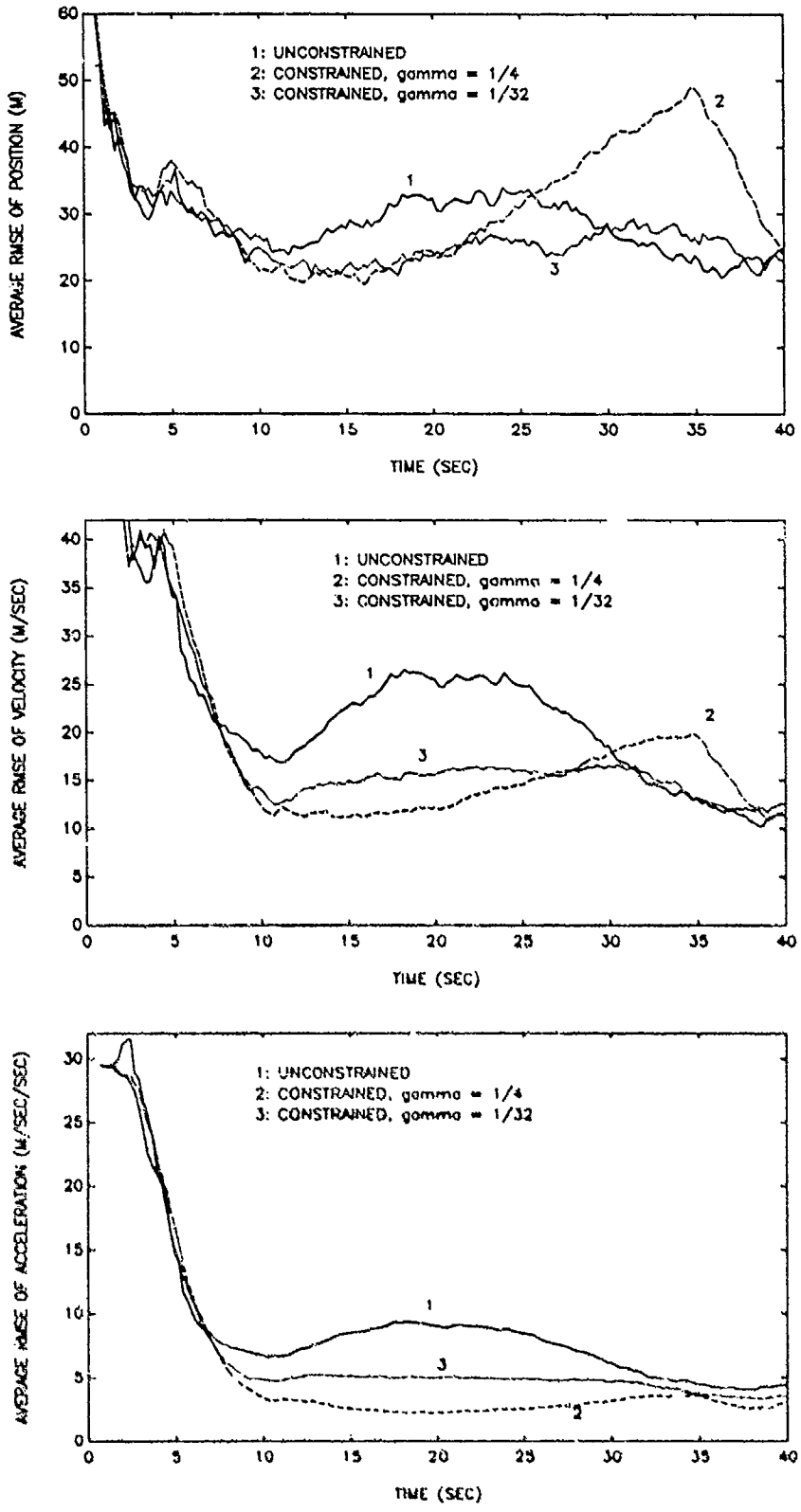

Figure 5.20 Effects of Deviations in Speed on the Kinematically Constrained Track Filter With 4 Hz Data, $q_k = 3$ m/sec^3, $\sigma_r = 8$ m, and $\sigma_b = \sigma_e = 2$ mrad

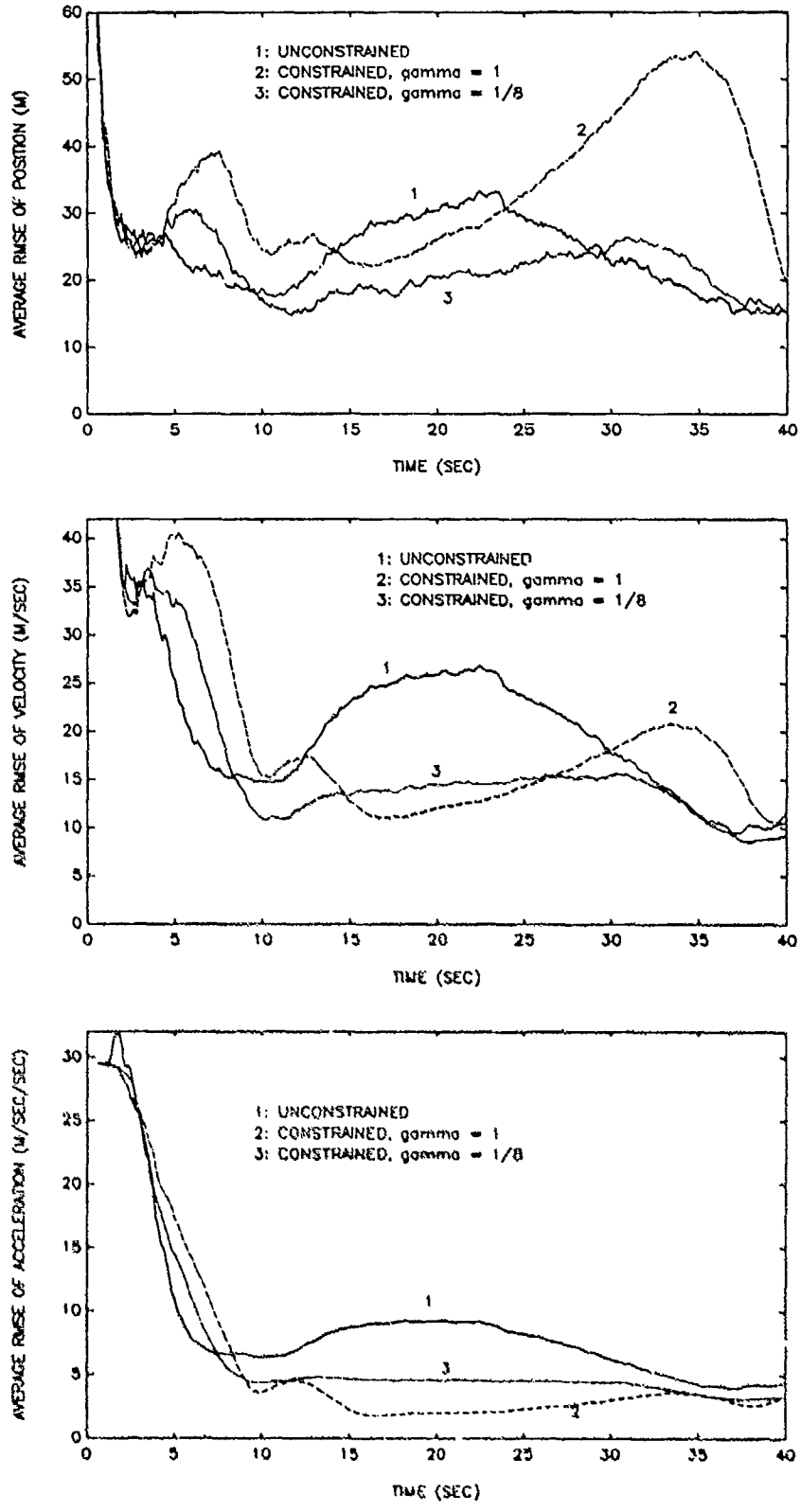

Figure 5.21 Effects of Deviations in Speed on the Kinematically Constrained Track Filter With 10 Hz Data, $q_k = 3$ m/sec^3, $\sigma_r = 8$ m, and $\sigma_b = \sigma_e = 2$ mrad

The improved state estimation accuracy obtained by including the kinematic constraint as a pseudomeasurement to a track filter has been demonstrated using the simulation results of this section. Improvement has been achieved for a variety of tracking conditions. The amount of improvement can be set by varying the constraint variance under the conditions described above. The target maneuvers chosen for the simulation results demonstrated that the kinematic constraint is useful in increasing tracking performance. Other targets similar to the decreasing speed target should be explored in depth to determine the amount of improvement that the kinematic constraint can provide and under which conditions when compared to its unconstrained counterpart. The accuracy of state estimates for maneuvering targets can be greatly improved by employing the kinematic constraint with this formulation.

CHAPTER 6
SUMMARY AND CONCLUSIONS

A new formulation of the kinematic constraint was presented, and the use of the kinematic constraint was shown through simulation results to improve the tracking of constant speed, maneuvering targets with a constant acceleration Kalman filter. Under the assumption of Eq. (4.40) the system with kinematic constraint was shown be uniformly completely controllable and uniformly completely observable which implies that the kinematically constrained filter is uniformly asymptotically stable. As discussed in Chapter 4, the sufficient condition of the assumption in Eq. (4.40) is not very restrictive in practice. The kinematically constrained filter was also shown to be unbiased. In addition, the lower bound of the covariance matrix of the kinematically constrained filter was shown to depend on a parameter γ defined in Eq. (4.40). In the filter design process, the parameter γ may be chosen so that this lower bound does not violate the Cramer-Rao lower bound.

While improvement in tracking performance was obtained with the kinematic constraint, a quantitative measure of the benefits gained by using the kinematic constraint as a pseudomeasurement are not clear at this time. The kinematic constraint used in this work is valid when the target is moving through a constant speed trajectory. While the parameter μ_k was introduced to relax the constraint, procedures for selecting the statistics of μ_k for the case of a variable speed target are not available at this time. As indicated by the simulation results, the use of the kinematic constraint improves the tracking performance only when the target is moving at a constant (or nearly constant) speed. An important issue is to identify the benefits of this constraint when the target is moving at a rather variable speed. While this issue has not been thoroughly addressed at this time, the Interacting Multiple Model (IMM) algorithm [10] provides a technique for utilizing a kinematically constrained filter for constant speed maneuvering targets in conjunction with other filter models for targets that maneuver with variable speed. Thus, additional research is needed to show the benefits and refine the method of implementation of the kinematic constraint. Also, methods for selecting R_k^μ *a priori* and during the tracking process are also needed.

REFERENCES

1. Singer, R.A., "Estimation of Optimal Tracking Filter Performance for Manned Maneuvering Target," *IEEE Trans. Aero. Elect. Sys.*, July, 1970, pp. 473–483.

2. McAway, R.J., and E. Delinger, "A Decision-Directed Adaptive Tracker," *IEEE Trans. Aero. and Elect. Sys.*, 1973, pp. 229–236.

3. Bar-Shalom, Y., and Birmiwal, K., "Variable Dimension Filter for Maneuvering Target Tracking," *IEEE Trans. Aero. and Elect. Sys.*, Sept. 1982, pp. 621–629.

4. Clark, B.L., *Development of an Adaptive Kalman Tracking Filter and Predictor for Fire Control Applications,* Naval Surface Warfare Center, Dahlgren, VA, NSWC TR–3445, 1977.

5. Berg, R.F., "Estimation and Prediction for Maneuvering Target Trajectories," *IEEE Trans. Auto. Cont.*, March 1983, pp. 294–304.

6. Alouani, A.T., Xia, P., Blair, W.D., and Rice, T.R., "A Two-Stage Kalman Estimator for State Estimation In the Presence of Random Bias and for Tracking Maneuvering Targets," *Proc. of 30th IEEE Conf. on Decision and Cont.*, Brighton, UK, Dec. 1991, pp. 2059–2062.

7. Chang, C.B., and Athans, M., "State Estimation for Discrete Systems with Switching Parameters," *IEEE Trans. Aero. and Elect. Sys.*, May 1978, pp. 418–425.

8. Chan, Y.T., Hu, A.G.C., and Plant, J.B., "A Kalman Filter Based Tracking Scheme with Input Estimation," *IEEE Trans. Aero. and Elect. Sys.*, March 1979, pp. 237–244.

9. Bogler, P.L., "Tracking a Maneuvering Target Using Input Estimation," *IEEE Trans. Aero. and Elect. Sys.*, May 1987, pp. 298–310.

10. Blom, H.A.P., and Bar-Shalom, Y., "The Interacting Multiple Model Algorithm for Systems with Markovian Switching Coefficients," *IEEE Trans. Auto. Cont.*, Aug. 1988, pp. 780–783.

11. Tahk, M., and Speyer, J.L., "Target Tracking Problems Subject to Kinematic constraints," *IEEE Trans. Auto. Cont.*, March 1990, pp. 324–326.

12. Stubberud, Seminar in Kalman Filtering, University of California, Irvine, University Extension, Oct. 15–17, 1990.

13. Jazwinsky, A. H., *Stochastic Processes Filtering Theory*, Academic Press, San Diego, CA, 1970.

14. McGarty, T. P., *Stochastic Systems and State Estimation*, John Wiley & Sons, New York, NY, 1974.

DISTRIBUTION

	Copies
ATTN DR RABINDER MADAN 1114SE CHIEF OF NAVAL RESEARCH 800 N QUINCY ST ARLINGTON VA 22217-5000	1
ATTN DR GLENN M SPARKS ANTHONY VIDMAR JR GOVERNMENT ELECTRONIC SYSTEMS DIVISION GENERAL ELECTRIC COMPANY MOORESTOWN NJ 08057	1 1
ATTN PROF YAAKOV BAR-SALOAM DON LERRO ESE DEPARTMENT U-157 260 GLENBROOK RD STORRS CT 06269-3157	1 1
ATTN OLIVER E DRUMMOND PH D PROFESSIONAL ENGINEER GENERAL DYNAMICS AIR DEFENSE SYSTEMS DIVISION 10900 E 4TH ST MZ 601-75 RANCHO CUCAMONGA CA 91730	1
ATTN DR J N ANDERSON A T ALOUANI P K RAJAN DEPARTMENT OF ELECTRICAL ENGINEERING TENNESSEE TECHNOLOGICAL UNIVERSITY TTU BOX 05004 COOKEVILLE TN 38505	1 5 1
ATTN DR GEORGE SWISHER COLLEGE OF ENGINEERING TTU BOX 05005 TENNESSEE TECHNOLOGICAL UNIVERSITY COOKEVILLE TN 38505	1
ATTN EDWARD PRICE SCOTT GODFREY FMC CORPORATION 1 DANUBE DR KING GEORGE VA 22485	1 1
ATTN JOSEPH S PRIMERANO RAYTHEON PO BOX 161 DAHLGREN VA 22448	1
ATTN DR RAGHAVAN LNK CORPORATION 6800 KENNELWORTH AVE STE 306 RIVERDALE MD 20737	1
ATTN GLENN WOODARD SYSCON CORPORATION TIDEWATER DIVISION PO BOX 1480 DAHLGREN VA 22448-1480	1
DEFENSE TECHNICAL INFORMATION CENTER CAMERON STATION ALEXANDRIA VA 22304-6145	2
INTERNAL DISTRIBUTION:	
E231	3
E232	2
E261 (GARNER)	1
E32 (GIDEP)	1
F21	1
F21 (PARKER)	1
F21 (RYAN)	1
F32 (HILTON)	1
F41	2
F41 (TANNER)	1
F41 (MARTIN)	1
F41 (KLOCHAK)	1

DISTRIBUTION (CONTINUED)

	Copies
F44	1
G	1
G05	1
G06	1
G07	1
G11 (DOSSETT)	1
G11 (GROVES)	1
G11 (LUCAS)	1
G13 (BEUGLASS)	1
G20	1
G23 (OHLENMEYER)	1
G23 (JOHN BIBEL)	1
G23 (MALYEVAC)	1
G43 (GRAFF)	1
G70	1
G702 (AUGER)	1
G706 (BUSCH)	1
G71	1
G71 (BLAIR)	30
G71 (RICE)	1
G71 (GRAY)	1
G71 (MURRAY)	1
G71 (CONTE)	1
G71 (WATSON)	25
G72 (GENTRY)	1
G72 (BOYKIN)	1
G73 (FONTANA)	1
N05	1
N05 (GASTON)	1
N24	1
N24 (BAILEY)	1
N24 (HANSEN)	1
N24 (SERAKOS)	1
N32 (CURRY)	1
N35 (BOYER)	1
N35 (HELMICK)	1
N35 (HARTER)	1
N35 (BAILEY)	1
N35 (FENNEMORE)	1

REPORT DOCUMENTATION PAGE

Form Approved
OMB No. 0704-0188

1. AGENCY USE ONLY *(Leave blank)*	2. REPORT DATE	3. REPORT TYPE AND DATES COVERED
	November 1991	

4. TITLE AND SUBTITLE
Use of Kinematic Constraint in Tracking Constant Speed Maneuvering Targets

5. FUNDING NUMBERS

6. AUTHOR(S)
W. D. Blair, G. A. Watson, and A. T. Alouani

7. PERFORMING ORGANIZATION NAME(S) AND ADDRESS(ES)
Naval Surface Warfare Center (Code G71)
Dahlgren, VA 22448-5000

8. PERFORMING ORGANIZATION REPORT NUMBER
NAVSWC TR 91-561

9. SPONSORING/MONITORING AGENCY NAME(S) AND

10. SPONSORING/MONITORING AGENCY REPORT NUMBER

11. SUPPLEMENTARY NOTES

12a. DISTRIBUTION/AVAILABILITY
Approved for public release; distribution is unlimited.

12b. DISTRIBUTION CODE

13. ABSTRACT *(Maximum 200 words)*

The use of a kinematic constraint as a pseudomeasurement in the tracking of constant speed maneuvering targets is considered in this report. The kinematic constraint provides additional information about the target motion that can be processed as a pseudomeasurement to improve tracking performance. The kinematic constraint for constant speed targets is $A \cdot V = 0$, where A and V are the target acceleration and velocity vectors, respectively. In previous publications, the measurement equation for processing the kinematic constraint as a pseudomeasurement was derived by a direct application of Taylor's theorem for a first order linearization of that pseudomeasurement equation. A new formulation of the constraint equation that provides significantly better tracking performance than the previous formulation is presented, and the rationale for the new formulation is discussed. The filter using the kinematic constraint for constant speed targets is shown to be unbiased and stochastically stable. Simulated tracking results are given to show the potential for further improving the performance of a track filter through the use of the proposed kinematic constraint. Simulation studies are presented for various data rates, levels of measurement errors, and deviations in speed.

14. SUBJECT TERMS	15. NUMBER OF PAGES
kinematic constraint, pseudomeasurement, constant speed targets	66
	16. PRICE CODE

17. SECURITY CLASSIFICATION OF REPORT	18. SECURITY CLASSIFICATION OF THIS PAGE	19. SECURITY CLASSIFICATION OF ABSTRACT	20. LIMITATION OF ABSTRACT
UNCLASSIFIED	UNCLASSIFIED	UNCLASSIFIED	UL

GENERAL INSTRUCTIONS FOR COMPLETING SF 298

The Report Documentation Page (RDP) is used in announcing and cataloging reports. It is important that this information be consistent with the rest of the report, particularly the cover and its title page. Instructions for filling in each block of the form follow. It is important to ***stay within the lines*** to meet ***optical scanning requirements.***

Block 1. Agency Use Only *(Leave blank).*

Block 2. Report Date. Full publication date including day, month, and year, if available (e.g. 1 Jan 88). Must cite at least the year.

Block 3. Type of Report and Dates Covered. State whether report is interim, final, etc. If applicable, enter inclusive report dates (e.g. 10 Jun 87 - 30 Jun 88).

Block 4. Title and Subtitle. A title is taken from the part of the report that provides the most meaningful and complete information. When a report is prepared in more than one volume, repeat the primary title, add volume number, and include subtitle for the specific volume. On classified documents enter the title classification in parentheses.

Block 5. Funding Numbers. To include contract and grant numbers; may include program element number(s), project number(s), task number(s), and work unit number(s). Use the following labels:

C	- Contract	**PR**	- Project
G	- Grant	**TA**	- Task
PE	- Program Element	**WU**	- Work Unit Accession No.

BLOCK 6. Author(s). Name(s) of person(s) responsible for writing the report, performing the research, or credited with the content of the report. If editor or compiler, this should follow the name(s).

Block 7. Performing Organization Name(s) and address(es). Self-explanatory.

Block 8. Performing Organization Report Number. Enter the unique alphanumeric report number(s) assigned by the organization performing the report.

Block 9. Sponsoring/Monitoring Agency Name(s) and Address(es). Self-explanatory.

Block 10. Sponsoring/Monitoring Agency Report Number. *(If Known)*

Block 11. Supplementary Notes. Enter information not included elsewhere such as: Prepared in cooperation with...; Trans. of...; To be published in.... When a report is revised, include a statement whether the new report supersedes or supplements the older report.

Block 12a. Distribution/Availability Statement. Denotes public availability or limitations. Cite any availability to the public. Enter additional limitations or special markings in all capitals (e.g. NOFORN, REL, ITAR).

DOD	- See DoDD 5230.24, "Distribution Statements on Technical Documents."
DOE	- See authorities.
NASA	- See Handbook NHB 2200.2
NTIS	- Leave blank

Block 12b. Distribution Code.

DOD	- Leave blank.
DOE	- Enter DOE distribution categories from the Standard Distribution for Unclassified Scientific and Technical Reports.
NASA	- Leave blank.
NTIS	- Leave blank.

Block 13. Abstract. Include a brief ***(Maximum 200 words)*** factual summary of the most significant information contained in the report.

Block 14. Subject Terms. Keywords or phrases identifying major subjects in the report.

Block 15. Number of Pages. Enter the total number of pages.

Block 16. Price Code. Enter appropriate price code ***(NTIS only)***

Block 17.-19. Security Classifications. Self-explanatory. Enter U.S. Security Classification in accordance with U.S. Security Regulations (i.e., UNCLASSIFIED). If form contains classified information, stamp classification on the top and bottom of this page.

Block 20. Limitation of Abstract. This block must be completed to assign a limitation to the abstract. Enter either UL (unlimited or SAR (same as report). An entry in this block is necessary if the abstract is to be limited. If blank, the abstract is assumed to be unlimited.